

2

N6TR -- 09/83

BR25/0562

# **LOW CARBON- MANGANESE- NICKEL-NIOBIUM- STEEL**



**COMPANHIA BRASILEIRA DE  
METALURGIA E MINERAÇÃO**

10



**COMPANHIA BRASILEIRA DE  
METALURGIA E MINERAÇÃO**

**Head Office**

Caixa Postal 8  
38180 Araxá, MG - Brazil  
Phone: (034) 661.1544 Telex: (034) 3355 CBMM BR

**Branch Offices**

**BRASIL**

Companhia Brasileira de Metalurgia e Mineração  
Rua Padre João Manoel, 923 - 9º andar  
01411 - São Paulo, SP - Brazil  
Phone: (011) 881.7100 Telex: (011) 25683 CBMM BR

**EUROPE**

Niobium Products Company GmbH  
Wagnerstrasse 4  
D-4000 Düsseldorf - 1 West Germany  
Phone: (211) 35.3404 Telex: (41) 8587006 NPC D

**NORTH AMERICA**

Niobium Products Company Ltd.  
440 Park West Bldg. Two  
Cliff Mines Road  
Pittsburgh, PA 15275 - U.S.A.  
Phone: (412) 787.9620 Telex: (230) 90.2936 NPC-PGH

**ORIENT**

CBMM Internacional  
Akasaka Brighton Bldg. 5th Fl  
5-2, Akasaka 1 - Chome, Minato-Ku  
Tokyo 107 - Japan  
Phone: (3) 586.3921 Telex: (72) 26616 CBMM J

# **LOW CARBON- MANGANESE- NICKEL-NIOBIUM- STEEL**

An alternative route to produce X65 to X75 pipeline grades applying relaxed rolling conditions

F. HEISTERKAMP and K. HULKA,  
Niobium Products Company GmbH

Besides the principle authors the following companies, institutes and metallurgists, have participated in this joint investigation:

British Gas Corp.	U.K.	Ph. Kirkwood
British Steel Corp.	U.K.	B. Morrison
"	U.K.	K. Randerson
Central Scientific Res. Inst. of Ferrous Metal.	U.S.S.R	I.I. Frantov
"	U.S.S.R	S.A. Golovanenko
"	U.S.S.R	D.A. Litvinenko
Falck S.A.	Italy	A. Molaroni
"	Italy	G. Pepi
Hoesch	Germany	B. Bersch
"	Germany	W. Haumaun
"	Germany	K. Kaup
"	Germany	R. Schröder
Klöckner-Werke	Germany	P. Brandscheid
Microalloying Int.	U.S.A.	J.M. Gray
Niobium Products Company Ltd.	U.S.A.	H. Stuart
Nuova-Italsider	Italy	A. Aprile
"	Italy	A. de Vito
Sheffield Univ.	U.K.	G.J. Davies
Sheffield Univ.	U.K.	S.R. Keown
Usinor	France	A. Coolen
"	France	M. Lafrance
Vallourec	France	M.J. Leca

## Contents

1 — Introduction .....	1
2 — Metallurgy of HSLA Steel Grades Containing Nickel and Niobium .....	2
3 — Investigation .....	3
4 — Results of the Investigation .....	4
4.1 — Mechanical Properties .....	4
4.2 — Internal Quality and Microstructure .....	8
4.3 — Precipitation Behaviour Based on Chemical Extraction Results .....	9
4.4 — Texture Evaluation .....	11
5 — Structure - Property Relationships .....	11
6 — Results of Weldability Investigations .....	12
6.1 — Welding Simulation .....	12
6.2 — Laboratory Welding .....	13
6.3 — Properties of Pipe Welds .....	13
7 — Summary and Conclusions .....	15
Literature .....	17

## TABLES AND FIGURES

Table 1 — Chemical composition of trial heats .....	4
Table 2 — Rolling conditions and mechanical properties of plate and strip production .....	6
Table 3 — Mechanical properties and results of chemical extraction analysis for a random selection of plates investigated .....	10
Table 4 — Chemical composition of welding consumables .....	12
Table 5 — Mechanical properties of produced pipes .....	13
Table 6 — Mechanical properties of actual CRC weldment .....	15
Fig. 1 — Yield point, tensile strength and transition temperature of a low carbon steel as a function of grain size .....	18
Fig. 2 — $A_{r_1}$ - Temperatures for 0.035% C-0.045% Nb-steels with various Ni and Mn-contents .....	19
Fig. 3 — Influence of Ni content on the transverse mechanical properties of normalized microalloyed LPG steel grades base composition: 0.09% C, 0.31% Si, 1.46% Mn, 0.015% P, 0.013% S, 0.038% Al, 0.07% Nb ..	20
Fig. 4 — Effect of niobium content on austenite grain size at 1175°C soaking temperature .....	21
Fig. 5 — Effect of niobium on critical reduction and temperature for austenite recrystallization .....	22
Fig. 6 — Influence of rolling conditions on the mechanical properties of plate and strip material, th. $\leq$ 17.5 mm	23
Fig. 7 — Influence of plate thickness on mechanical properties for different rolling conditions (soaking temperature $\approx$ 1200°C) .....	24

Fig. 8 — Correlation between CVN and BDWT test results . . . .	25
Fig. 9 — Correlation between strength, toughness, grain refinement and precipitation hardening for 17.5 mm plates . . . . .	26
Fig. 10 — Ductility properties of Ni Nb-plates . . . . .	27
Fig. 11 — Form of yield point and influence of annealing (600°C/30 min.) (transverse) . . . . .	28
Fig. 12 — Niobium carbide inclusions in eutectic formation (ZnSe coated) . . . . .	29
Fig. 13 — Microstructure of Ni Nb steel plates after various rolling conditions . . . . .	30
Fig. 14 — Influence of rolling conditions on the average ferrite grain size . . . . .	31
Fig. 15 — Examples for Nb(C,N) precipitates with different particle size - a) about 2000 Å - b) about 200 Å - c) about 20 Å - d) about 40 Å (transmission electron microscope, replica technique) . . . . .	32
Fig. 16 — Influence of rolling conditions on soluble nitrogen and soluble niobium content . . . . .	33
Fig. 17 — Comparison of free nitrogen content evaluated by chemical extraction and by hydrogen extraction technique . . . . .	34
Fig. 18 — Correlation between ferrite grain size and CVN-FATT	35
Fig. 19 — Correlation between ferrite grain size and yield strength	36
Fig. 20 — Correlation between soluble niobium content and yield strength increase . . . . .	37
Fig. 21 — CCT - Diagram of Ni Nb steel after austenitizing at 1350°C . . . . .	38
Fig. 22 — Influence of cooling rate on impact toughness of simulated heat affected zone of Ni Nb steel (peak temp.: 1350°C) . . . . .	39
Fig. 23 — Toughness of Ni Nb spiral pipe weld metal for various wire composition (Laboratory Welding) . . . . .	40
Fig. 24 — Toughness of Ni Nb spiral weldment (16 mm) (Laboratory Welding) . . . . .	41
Fig. 25 — Toughness of Ni Nb spiral pipe . . . . .	42
Fig. 26 — Microstructure of Ni Nb spiral pipe (S2 TiMoB wire, Lincoln 790 flux) . . . . .	43
Fig. 27 — Toughness properties of Ni Nb - UO - pipes . . . . .	44
Fig. 28 — Toughness properties of Ni Nb - UO - pipe (56 inch × 17.5 mm, transverse) . . . . .	45
Fig. 29 — Microstructure of circumferential weldment of Ni Nb steel (spiral pipe) . . . . .	46
Fig. 30 — Notch toughness and hardness distribution in circumferential weldment of Ni Nb spiral pipe . . . . .	47
Fig. 31 — Hardness distribution in CRC-cross weldment of Ni Nb pipe (as welded) . . . . .	48

*ABSTRACT — Experimental heats of a low carbon-manganese-0.5% nickel-0.15% niobium-steel have been rolled to plates between 13.5 and 50 mm thickness and to a 16 mm hot strip. Various combinations of soaking temperatures from 1100°C to 1300°C and of finish rolling temperatures between 710°C and 930°C have been investigated.*

*From the mechanical properties obtained, one can conclude that the investigated steel composition provides very good properties e.g. for pipe line steels X65 to X75. In particular the toughness at low temperature is outstanding despite relaxed rolling conditions.*

*Metallographic and special investigations such as electron microscopy, texture evaluation and chemical extraction, correlated with applied rolling schedules and the mechanical properties obtained resulted in a comprehensive understanding about the benefits of high niobium metallurgy combined with nickel addition.*

*All practically applied welding processes generated mechanical properties, in particular toughness of the weldment, that meet arctic specifications.*

## 1 - Introduction

Rising energy consumption has brought a steady increase in construction of new pipelines all over the world, including arctic and submarine regions. Modern pipeline engineering calls for pipes having higher transportation capacity, improved weldability and safety. Consequently, during the last 25 years there has been a continuous development in pipeline steel grades. Nowadays, the most relevant product for large diameter pipes is Grade X70, produced by thermo-mechanical treatment of pearlite-reduced, microalloyed steels.

Basically, two types of Grade X70 are applied, both relying on niobium to provide a fine-grained microstructure, especially due to its effect on the retardation of austenite recrystallization during rolling. The precipitation-hardening type, with a typical carbon content of approximately 0.10%, applies niobium along with other microalloying elements, such as vanadium or titanium, which guarantee the required strength as a result of fine carbonitride or carbide precipitation in ferrite. The other type, acicular ferrite X70 steel, achieves its additional strength by dislocation hardening and cold working during pipe making.

The transformation temperature of this steel is mainly reduced by alloying with approximately 0.30% molybdenum. For a good ratio of strength to toughness, the carbon content of this steel grade has to be reduced to well below the 0.1% level.

The general target in steel development is, however, to find the most economic solution to meet all technical requirements. In this context, all costs — steelmaking, alloying and rolling — have to be taken into consideration. It is the aim of this investigation to show an alternative route to existing steel grades for the production of X65/X75 linepipe steel.

## 2 - Metallurgy of HSLA Steel Grades Containing Nickel and Niobium

Pipeline steel grades are strengthened by several mechanisms. Of these, solid-solution, dislocation and precipitation hardening impair the fracture appearance transition temperature, FATT, whereas grain refinement improves both yield strength and toughness, Fig. 1.<sup>(1)</sup>

In this context, nickel plays a specific role. Besides a moderate increase in yield and tensile strength, resulting from solid solution hardening, about 30 N/mm<sup>2</sup> per wt% of nickel,<sup>(2)</sup> it mainly acts by reducing the  $\gamma$  -  $\alpha$  transformation temperature. Under continuous cooling conditions, the  $A_{r3}$  temperature for a carbon-reduced microalloyed steel grade with 1.5%Mn is lowered by about 50°C per 1.0%Ni,<sup>(3)</sup> Fig. 2. Therefore, Ni alloyed ferritic steel grades show a finer grain size and correspondingly improved toughness.

Nickel-alloyed ferritic steels are widely used in structural application<sup>(4)</sup> and are usually normalized. The main application, using nickel contents of about 0.7%, is for cryogenic construction such as tankers and storage tanks for liquid gases (LPG). Other ferritic steels for service temperatures down to -196°C use nickel contents up to 9%. Besides the mentioned nickel-alloyed steels, there are also pearlite reduced niobium microalloyed grades in the normalized condition which fulfill the requirements for LPG construction. These steels have better toughness and strength if a controlled rolling process is applied before normalizing.<sup>(5)</sup>

The combination of nickel plus niobium results in further improvements in toughness up to Ni contents which still allow transformation into a ferrite-pearlite microstructure, Fig. 3.<sup>(6)</sup> The occurrence of either bainite or martensite usually impairs toughness.

For the production of pipeline steel grades, the role of the alloying elements during thermomechanical processing is of particular interest.

At present, niobium is widely added to pipeline steels up to levels of 0.06%. However, special benefits obtained with higher contents will be illustrated briefly.



With higher niobium contents, a significant number of undissolved carbonitride particles can be obtained at usual soaking temperatures. These particles when exhibiting the proper size and distribution<sup>(7)</sup> effectively contribute to produce a finer austenite grain, Fig. 4.<sup>(8)</sup> Since the critical deformation for austenite recrystallization is reduced by a finer grain size, it can be anticipated that a higher niobium steel, for most practical rolling schedules, will exhibit enhanced grain refinement after finish roughing.

After the roughing stage, the characteristic feature of thermo-mechanical processing is the application of a certain amount of deformation in the non recrystallization range of austenite. This results in elongated austenite grains, with large grain boundary areas and deformation bands which, naturally, transform into finer ferrite grains.

Since the temperature when retardation of austenite recrystallization is firstly observed increases with the niobium content, Figs. 5a<sup>(9)</sup> and 5b<sup>(10)</sup>, a much more effectively refined ferrite grain size can be achieved - for a given rolling schedule - when higher niobium contents are used. Or on the other hand, either a reduced deformation at low rolling temperatures or a higher finishing temperature can be used to obtain a defined grain size. In summary, a less controlled rolling schedule is obtained.

It should also be mentioned that the part of the niobium remaining dissolved in austenite is able to contribute to strength increase by precipitation hardening of ferrite. In turn, the amount of precipitation hardening in ferrite is inversely correlated with the severity of the deformation schedule which controls prior precipitation in austenite.

Regarding these metallurgical correlations, one can expect that greater niobium contents, together with the effect of nickel alloying, guarantee comparable properties when less severe rolling schedules are used. Furthermore, the combined addition of nickel and niobium acts not only on grain refining but also on precipitation hardening. By reducing the  $A_{r3}$ -temperature, nickel promotes an evenly distribution of niobium carbonitride precipitation in ferrite<sup>(11)</sup>. On the other hand, for a given temperature, the precipitation of carbides and nitrides is promoted by nickel. Therefore, the precipitates will be comparatively coarser when compared to a Ni-free grade. Thus, dislocations follow loops between precipitates resulting in the development of a more homogeneous distribution of slip planes within the grains and smaller slip steps at the grain boundaries.<sup>(12)</sup>

### 3 - Investigation

In view of the above technical considerations, it was deemed appropriate to carry out a full scale test. As a result, two trial heats of a low C-Mn-Ni steel having 0.11 and 0.13% nominal niobium content have been produced at Nuova-Italsider's Taranto Works. The

chemical compositions of these heats are given in Table 1. The alloy design includes the maximum amount of manganese plus nickel that still allows transformation to a ferrite-pearlite microstructure.

Slabs of both heats have been rolled at Taranto Works under different rolling schedules incorporating variations in soaking temperature, time-temperature-deformation schedule, final plate thickness and finish rolling temperature. In addition, slabs of Heat B have been distributed to several companies in Europe and have been rolled under different rolling schedules to plate and strip.

Mechanical properties and microstructure have been evaluated at each company. Selected specimens of the material have also been used to evaluate microstructure, precipitation behaviour by chemical extractions and mobile nitrogen, as well as for texture determination and to conduct special investigations using electron microscopy.

Weldability of the experimental steel has been investigated in laboratory trials and in full-scale mill production of pipes (U-O-pipe and spiral pipe).

#### 4 - Results of the Investigation

##### 4.1 - Mechanical Properties

For each plate or strip produced, the rolling conditions and mechanical properties (transverse direction) are given in Table 2. These data have been summarized in two diagrams (Figures 6 and 7) which show the correlation with finish rolling temperature and plate thickness. It should be noted that a lower finishing temperature in most cases also corresponds with a higher amount of total deformation in the unrecrystallized austenite region. Slabs of Heat A had a greater starting thickness (280 mm), therefore, the total deformation was larger, particularly in the first stages of rolling.

It is most remarkable that independent of the company where the material has been rolled, all results fit into one, rather narrow, scatterband.

For 17.5 mm plate, the tensile properties after rolling at temperatures  $\geq 820^{\circ}\text{C}$  are sufficient for Grade X65. With lower rolling temperatures, strength increases exponentially. This is more pronounced for yield strength, therefore, the Re/Rm ratio is higher at reduced

**Table 1 - Chemical Composition of Trial Heats**

Chemical Composition in %								
Heat	C	Si	Mn	P	S	Al	Ni	Nb
A	0.075	0.43	1.58	0.013	0.005	0.021	0.51	0.106
B	0.077	0.36	1.56	0.017	0.005	0.020	0.47	0.130

FRT (Finish Rolling Temperature). While soaking temperature had no evident influence on the properties of Heat B, higher soaking temperature resulted in higher tensile properties for Heat A.

Thinner plates show comparable higher yield strengths and strip production with accelerated cooling plus coiling results in properties comparable with properties for plates finished at temperatures about 100°C lower. These approaches represent two possibilities to reach X75 properties with the present steel grade.

The 17.5 mm plates of Heat B show comparable higher tensile properties than plates from Heat A. This is particularly evident for thicker plates (Figure 7). More severe rolling at low temperature resulted in higher yield strength in plates  $\geq 20$  mm in the case of Heat A. This effect was not observed in Heat B. In general, tensile properties are lowered with increasing plate thickness in the range of approximately 2 N/mm<sup>2</sup> per mm plate thickness.

It should be mentioned that all specimens showed discontinuous yielding behaviour. Consequently, the values reported for Re, Rp 0.2 or Rp 0.5 are equivalent.

Regarding toughness, more complex correlations with the processing conditions are found. Finish rolling temperatures  $> 880^{\circ}\text{C}$  result in inadequate transition temperature of 0 to 20°C for 50% CVN (Charpy V-Notch) shear fracture. Much better results are achieved at lower finishing temperatures and higher total deformation below 900°C.

The influence of finish rolling temperature is different for high (approximately 1300°C) and low (approximately 1100°C) soaking temperatures, especially for plates thinner than 17.5 mm. While improved FATT (Fracture Appearance Transition Temperature) is achieved with lower finishing temperatures after soaking at 1100°C, the same practice impairs FATT after 1300°C soaking. Thinner plates and coil production result in much better toughness. For plates thicker than 20 mm, both a low finish rolling temperature and a large amount of deformation in the non-recrystallization range of austenite is necessary to achieve sufficient toughness. This is particularly noticeable for Heat A, whereas the properties of plates of Heat B seem to be more independent of the final rolling conditions.

In all cases, where good CVN toughness was obtained, the BDWT (Battelle Drop Weight Tear) test resulted in good toughness properties. Fig. 8 demonstrates that within a reasonable scatterband the BDWT temperature is approximately 25°C higher than the CVN-FATT, independent of chemical composition and plate thickness. The absolute values of BDWT temperature with results down to - 80°C for 85% shear fracture can be considered excellent.

All mechanical properties results can be analysed in terms of grain refinement and precipitation hardening factors. For the 17.5 mm plates,

Table 2: Rolling Conditions and Mechanical Properties of Plate and Strip Production.

Heat	Specimen Number	Slab Thickness mm	Soaking Temp. °C	Rolling Schedule	Final Thickness mm	Finish Temp. °C	Mech. Properties - Transverse		
							Re/Rp 0.5 N/mm <sup>2</sup>	Rm N/mm <sup>2</sup>	50% CVN FATT °C
A	1	280	1100	3 times below 800°C	17.5	750	487	565	-100
A	2	280	1100	3 times below 800°C	17.5	740	529	568	-100
A	3	280	1100	4 times below 800°C	17.5	760	491	532	-90
A	4	280	1100	continuous	17.5	820	447	536	-70
A	5	280	1100	3 times below 900°C	17.5	800	462	551	-65
A	6	280	1300	3 times below 800°C	17.5	740	559	614	-20
A	7	280	1300	3 times below 800°C	17.5	730	550	607	-40
A	8	280	1300	3 times below 900°C	17.5	790	500	584	-40
A	9	280	1300	4 times below 900°C	17.5	810	480	557	-60
A	10	280	1200	continuous	20.0	920	437	557	0
A	11	280	1200	continuous	20.0	900	435	569	0
A	12	280	1200	continuous	20.0	800	456	564	-60
A	13	280	1200	1.5 times below 850°C	20.0	780	449	550	-50
A	14	280	1200	2.5 times below 900°C	20.0	810	442	542	-60
A	15	280	1200	4 times below 900°C	20.0	800	480	549	-60
A	16	280	1200	continuous	30.0	920	430	550	+10
A	17	280	1200	continuous	30.0	930	415	552	+20
A	18	280	1200	continuous	30.0	770	460	535	-40
A	19	280	1200	2 times below 850°C	30.0	780	474	583	-10
A	20	280	1200	1.5 times below 850°C	30.0	790	425	531	-20
A	21	280	1200	continuous	40.0	920	406	529	0
A	22	280	1200	continuous	40.0	930	413	538	+10
A	23	280	1200	1.5 times below 900°C	40.0	810	415	536	+10
A	24	280	1200	3.5 times below 850°C	40.0	780	450	525	-50
A	25	280	1200	1.3 times below 850°C	50.0	770	398	517	-10
A	26	280	1200	1.2 times below 850°C	50.0	800	404	521	+10
A	27	280	1200	2 times below 900°C	50.0	830	432	533	-20

Table 2: Rolling Conditions and Mechanical Properties of Plate and Strip Production.

Heat	Specimen Number	Slab Thickness mm	Soaking Temp. °C	Rolling Schedule	Final Thickness mm	Finish Temp. °C	Mech. Properties - Transverse		
							Re/Rp 0.5 N/mm <sup>2</sup>	Rm N/mm <sup>2</sup>	50% CVN FATT °C
B	1	200	1100	3 times below 800°C	17.5	720	579	608	-90
B	2	200	1100	3 times below 800°C	17.5	740	575	611	-60
B	3	200	1100	3 times below 800°C	17.5	710	595	626	-100
B	4	200	1100	3 times below 900°C	17.5	780	513	570	-60
B	5	200	1100	3 times below 900°C	17.5	800	484	552	-80
B	6	200	1100	3 times below 900°C	17.5	800	484	576	-70
B	7	200	1300	3 times below 800°C	17.5	740	535	617	-25
B	8	200	1300	3 times below 800°C	17.5	760	526	615	-20
B	9	200	1300	3 times below 800°C	17.5	750	538	601	-40
B	10	200	1300	4 times below 900°C	17.5	810	462	557	-60
B	11	200	1300	3 times below 900°C	17.5	830	488	572	-50
B	12	200	1300	continuous	17.5	820	468	564	-50
B	13	200	1200	continuous	17.5	880	451	569	0
B	14	200	1200	continuous	17.5	900	460	594	+15
B	15	200	1200	continuous	17.5	890	463	597	+15
B	16	200	1200	continuous	17.5	920	461	586	+20
B	17	200	1200	4 times below 850°C	20.0	710	526	579	-60
B	18	200	1200	continuous	20.0	710	493	563	-60
B	19	200	1200	continuous	40.0	780	454	526	-60
B	22	200	1200	3.5 times below 850°C	40.0	730	442	515	-60
B	21	200	1200	continuous	40.0	720	455	532	-40
B	20	200	1200	2.5 times below 850°C	50.0	780	458	542	-60
B	23	200	1200	continuous	50.0	790	427	523	-55
B	24	200	1200	continuous	50.0	740	421	510	-65
B	25	200	1220	3 times below 900°C	20.0	760	501	565	-60
B	26	200	1220	3 times below 900°C	20.0	770	516	584	-55
B	27	200	1220	3 times below 900°C	25.0	700	512	578	-65
B	28	200	1250	coil outside, c.t. 620°C	16.0	810	575	632	-100
B	29	200	1250	coil middle, c.t. 520°C	16.0	790	582	640	-100
B	30	200	1250	coil inside, c.t. 600°C	16.0	790	598	666	-90
B	31	170	1150	continuous	13.5	850	521	580	-105
B	32	170	1250	2 times below 950°C	13.5	860	512	575	-110
B	33	200	1250	4 times below 900°C	17.5	760	496	590	-70
B	34	200	1150	4 times below 950°C	17.5	800	478	555	-75
B	35	200	1250	4 times below 950°C	15.0	810	513	571	-80
B	36	200	1250	4 times below 850°C	15.0	710	595	657	-75
B	37	200	1250	4 times below 850°C	15.0	720	611	652	-65
B	38	200	1250	4 times below 950°C	15.0	800	519	587	-65

this is shown in Fig. 9. Plates of Heat A austenitized at 1100°C show properties which follow a slope for grain refinement as finish rolling temperature is lowered. Plates of Heat B seem to be finer-grained and show properties which lead to the conclusion that more precipitation hardening is involved. This is more evident for plates finished below 800°C. The latter observation is also evident for all plates soaked at 1300°C, independent of the chemical composition. For these rolling conditions, even a low finish rolling temperature does not result in a finer-grained material. Continuously rolled plates with finishing temperatures of approximately 900°C have the coarsest grain sizes as anticipated and shown in Table 2. Since, in this case, little deformation is applied in the temperature range of maximum precipitation in austenite, precipitation hardening is high and of a similar order of magnitude to that in plates controlled-rolled below 800°C with 1300°C soaking temperature.

The ductility of all plates is excellent. Fig. 10 shows, for a complete selection of plates encompassing the whole range of different rolling conditions and plate thicknesses, that independent of chemical composition, the known correlations between elongation, reduction of area, CVN shelf energy and tensile strength, are obeyed.

For the same group of specimens, the yielding behaviour has been more closely examined. From Fig. 11 it can be observed that all specimens show Lüders elongation with a maximum of 4.5% for medium finishing temperatures. The scatterband for the dependence of yield strength on finish rolling temperature is predictably broad due to the variety of plate rolling conditions used and furthermore, the plot includes the whole range of rolling conditions with varying soaking temperature, plate/slab thickness, total deformation and coiling conditions.

It is interesting to note that a subcritical annealing treatment at 600°C for 30 minutes results in a higher yield strength for plates with finishing temperatures above 900°C as it will be discussed later. After annealing, the values of Lüders elongation for all plates become more uniform with the maximum occurring at a FRT of approximately 820°C. This maximum corresponds to the greatest difference between upper and lower yield strengths.

#### *4.2 - Internal Quality and Microstructure*

Good cleanness for plates and strips produced has been obtained. In most specimens, A2 sulfides and alumina or other oxides, B2 and D2 respectively, according to ASTM E 45/63, have been identified. In addition, small yellow inclusions in eutectic formation have been found, Fig. 12. Electron beam microanalysis of larger particles of this type indicated 91.7% niobium and 8.3% carbon. This result is very close to the stoichiometric composition of Nb<sub>4</sub>C<sub>3</sub> with 91.2% niobium

and 8.8% carbon. No nitrogen was found in these eutectic particles and it is thus concluded that they are niobium carbide.

The microstructure is mainly ferrite plus pearlite, but in some cases, Widmanstätten structure is observed, sometimes with small amounts of bainite. Examples of the microstructural changes with rolling conditions are presented in Figure 13.

For selected specimens, the ferrite grain size has been determined by the method of mean linear intercept. The main factor influencing achievement of a fine grain size is a low finishing temperature, Fig. 14, but rolling to thinner plates or strip rolling conditions generated a fine grained microstructure even at medium finishing temperatures.

Transmission electron microscopy showed that several types of Nb(C,N) precipitates are present. Examples for specimens B3, B29 and B36 are shown in Fig. 15 (Table 2). The distributions are described as follows:

- a) B3: Relatively coarse particles of about 2000 Å. These either remained undissolved during reheating, or were precipitated during rolling in the upper austenite region. The precipitates were found mainly in specimens soaked at temperatures of 1100 or 1200°C.
- b) B29: Particles of approximately 200 Å precipitated in the lower austenite range or in the  $\gamma + \alpha$  region. The precipitates are oriented in lines and are mainly found in specimens rolled below 900°C.
- c) B29: Very fine precipitates of about 20 Å and smaller (precipitation in ferrite) have been found in all specimens.
- d) B36: There is a large volume fraction of very homogeneously distributed precipitates of approximately 30 to 50 Å. For rolling conditions such as finish roughing at 1070°C, hold, start finish rolling at 830°C, FRT of 710°C, it is conceivable that these precipitates are strain induced and formed in the metastable austenite region. The low  $\gamma - \alpha$  transformation temperature of the steel would limit subsequent precipitate coarsening.

#### *4.3 - Precipitation Behaviour Based on Chemical Extraction Results*

A well known method for isolating carbonitrides in microalloyed steels is by the use of methanol iodide extraction. With this method, most of the precipitates remain undissolved. However, the very small particles deriving from precipitation in ferrite, might not be retained in the filtration residue. Therefore, the term "soluble" niobium represents the amount of niobium that remained in solid solution or, to a large extent, was finely precipitated in ferrite. By using the same method, insoluble and soluble nitrogen can also be determined. Aluminium nitride is in the isolate of the methanol iodide extraction and can be taken into solution by use of 50% NaOH, which does not influence the niobium carbonitride<sup>(14)</sup>.

**Table 3: Mechanical Properties and Results of Chemical Extraction Analysis for a Random Selection of Plates Investigated.**

Spec. No.	Mechanical Properties - Transverse direction												Chemical Extraction					Mobile N ppm	Average Ferrite Grain Size $\mu\text{m}$
	As-rolled						Annealed						Nb total %	Nb soluble %	N total %	N AlN %	N soluble %		
	Re <sup>H</sup> N/mm <sup>2</sup>	Re <sup>L</sup> N/mm <sup>2</sup>	R <sub>m</sub> N/mm <sup>2</sup>	A <sub>1</sub> %	A <sub>2</sub> %	Z %	Re <sup>H</sup> N/mm <sup>2</sup>	Re <sup>L</sup> N/mm <sup>2</sup>	R <sub>m</sub> N/mm <sup>2</sup>	A <sub>1</sub> %	A <sub>2</sub> %	Z %							
A 2	487	474	573	3.7	28	62.8	471	459	558	3.8	32	60.3	0.151	0.012	0.0068	0.0017	0.0012	7.8	
A 4	441	425	523	3.8	32	66.4	433	415	515	4.1	36	68.7	0.155	0.006	0.0069	0.0014	0.0013	9.5	
A 8	471	471	612	1.5	26	55.2	525	502	594	3.5	24	57.7	0.156	0.016	0.0066	0.0017	0.0009	8.2	
A 10	441	441	576	1.2	28	67.5	487	471	573	2.8	28	66.4	0.152	0.019	0.0062	0.0018	0.0014	7	12.0
A 14	461	446	545	3.3	32	68.7	459	438	538	3.9	34	66.4	0.147	0.007	0.0060	0.0021	0.0007	10.5	
A 22	420	408	525	2.7	32	69.8	469	446	553	2.8	30	68.7	0.144	0.014	0.0062	0.0018	0.0010	6	13.5
A 23	431	410	525	2.7	30	70.8	428	410	512	3.4	34	73.0	0.150	0.012	0.0063	0.0018	0.0011	13.0	
A 27	436	420	525	3.3	34	71.8	471	446	550	3.0	32	68.7	0.141	0.008	0.0063	0.0017	0.0009	6	14.0
B 3	520	504	576	4.3	28	61.5	504	489	563	4.5	34	53.8	0.168	0.034	0.0064	0.0013	0.0009	3	5.6
B 6	479	484	576	4.0	28	63.9	502	471	558	4.2	32	66.4	0.169	0.020	0.0065	0.0013	0.0011	8.6	
B 9	517	517	617	2.8	28	56.4	530	507	596	3.8	32	59.0	0.173	0.037	0.0069	0.0018	0.0010	10.0	
B 11	492	474	599	2.0	26	55.2	510	484	587	3.1	30	60.3	0.179	0.032	0.0071	0.0019	0.0009	11.0	
B 12	558	522	624	2.6	26	56.4	553	532	614	3.6	28	61.5	0.151	0.019	0.0061	0.0013	0.0010	12.0	
B 14	469	461	599	1.5	28	61.5	489	484	594	2.8	30	61.5	0.164	0.036	0.0067	0.0012	0.0014	8	13.0
B 16	464	464	599	1.2	28	62.8	497	482	589	2.7	28	61.5	0.173	0.024	0.0064	0.0019	0.0017	16.0	
B 29	571	563	650	2.1	25.2	61	608	597	640	5.0	25.0	59	0.160	0.029	0.0065	0.0018	0.0013	7	4.8
B 32	530	507	586	3.5	30.1	74	514	501	574	3.8	30.9	73	0.169	0.016	0.0057	0.0016	0.0008	5	5.4
B 35	523	506	586	3.6	28	61	505	493	572	3.3	26.4	62	0.169	0.021	0.0072	0.0019	0.0008	6	6.8
B 36	577	566	643	2.7	23.4	60	567	549	632	2.3	21.2	59	0.168	0.029	0.0068	0.0017	0.0006	6.5	
B 37	600	581	655	2.5	23.5	59	576	567	642	2.4	21.9	59	0.170	0.032	0.0065	0.0017	0.0005	3	7.2
B 38	517	499	572	3.6	28.9	61	498	484	559	3.0	28.0	63	0.168	0.018	0.0065	0.0016	0.0005	—	



Table III indicates that the total niobium content, evaluated by the above process, was always higher than that of the ladle analysis.

With regard to the various rolling conditions, Fig. 16, it can be seen that Heat B, having the higher niobium content, consistently shows a greater amount of soluble niobium. However, Heat A has a much greater slab thickness and, other things being equal, must therefore experience a higher total deformation. The result is an increased strain induced precipitation in the upper austenite region. Rolling conditions with finishing temperatures of 800 to 850°C result in less soluble niobium than rolling schedules avoiding this rapid precipitation region. Within the scatterband of these results, plates with 1100°C soaking temperature show the lowest values of soluble niobium.

For most plates, the range of soluble nitrogen contents of 0.0005 to 0.0012% is very low. Only plates with finishing temperatures above 900°C showed a higher content of soluble nitrogen.

Another method for determining soluble or mobile nitrogen involves heating steel turnings in pure hydrogen at 450°C. Mobile nitrogen will diffuse out of the steel and can be determined by the amount of ammonia produced. Results using this nitrogen extraction technique suggest that the mobile nitrogen is even lower than soluble nitrogen determined via the chemical extraction method, Fig. 17.

#### 4.4 - Texture Evaluation

A few specimens have been investigated at the University of Sheffield, using the method of orientation distribution functions (ODF).

Rolling conditions incorporating no severe deformation at low temperatures did not show heavily preferred orientation. The specimens B32 and B35 (Table 2) exhibited a maximum function height of 2.3 and 2.5 times random with the relatively weak components:  $\{001\}\langle 110\rangle$ ,  $\{001\}$  or  $\{111\}\langle uvw\rangle$ .

Specimens having a high degree of deformation at low temperatures, such as specimens B29 and B36 showed the typical texture resulting from  $\gamma - \alpha$  transformation from non-recrystallized austenite in which the main component is  $\{112\}\langle 110\rangle$  and with a weak  $\{001\}\langle 100\rangle$  contribution. The maximum function height of these specimens B29 and B36 is 3.2 and 3.9 respectively. This result demonstrates that even the low FRT of 710°C was fully in the austenite region because no  $\{100\}\langle uvw\rangle$  - texture, typically found in deformed or recrystallized ferrite, has been detected.

### 5 - Structure - Property Relationships

It has been shown that different rolling conditions influence microstructure, precipitation behaviour and mechanical properties.

The slope of the transition temperature - ferrite grain size plot follows very well the Hall-Petch-equation<sup>(15)</sup>, Fig. 18. The scatterband of the results can be explained in terms of the different strength levels, different amounts of precipitation hardening and varying free nitrogen levels. Specimens showing Widmanstätten structure or bainite islands fit into a higher temperature band (impaired FATT). The results of yield strength actually follow a  $d^{-1/2}$  correlation<sup>(16)</sup>, Fig. 19. The deviation from this equation shows a good correlation with the soluble niobium content, Fig. 20. The regression formula of this plot indicates that 0.01% of "soluble" niobium cause a yield strength increase of approximately 30 N/mm<sup>2</sup>. This value corresponds to niobium carbonitride precipitates having a diameter of approximately 20 Å (17). It thus appears that nearly all the "soluble" niobium content exists in the form of precipitates in ferrite. It should be noted that the constant for the regression equation, Fig. 20, includes, among others, the influence of texture and coarser niobium precipitates formed in the austenite region.

## 6 - Results of Weldability Investigations

### 6.1 - Welding Simulation

The simulation of the weld HAZ includes evaluation of microstructure and of Charpy impact energy for various cooling rates after austenitizing to a peak temperature of 1350°C<sup>(18)</sup>.

The continuous cooling transformation diagram is shown in Fig. 21. It can be seen that the martensite transformation occurs outside the limits of cooling rates between 70 and 100°C/s for manual arc welding, which can be reached during pipe laying in winter. Consequently, the steel investigated has no tendency for cold cracking. The steel grade shows a wide zone of bainitic transformation, with the formation of ferrite limited to cooling rates < 3.5°C/s.

The results of impact testing illustrated in Fig. 22 show that the nickel niobium steel is suitable for welding within the range of heat

**Table 4 - Chemical Composition of Welding Consumables**

Wire	C	Si	Mn	P	S	Al	Ni	Mo	Ti	B
S2Mo	0.12	0.13	1.00	0.013	0.014	0.008	—	0.54	—	—
S3	0.12	0.10	1.52	0.012	0.023	0.002	—	0.02	—	—
S2TiMo (AS42)	0.11	0.20	1.03	0.013	0.004	0.012	—	0.47	0.16	—
S2 TiMoB	0.10	0.20	1.05	0.014	0.004	0.012	—	0.02	0.08	0.008
Cel 80	0.19	0.12	0.85	0.014	0.012	0.007	0.26	0.08	—	—
K-Nova	0.09	0.57	1.30	0.014	0.018	0.009	—	0.02	0.01	—
Flux	SiO <sub>2</sub>	CaO	MnO	Fe <sub>2</sub> O <sub>3</sub>	Al <sub>2</sub> O <sub>3</sub>	TiO <sub>2</sub>	MgO	CaF <sub>2</sub>	B <sub>2</sub> O <sub>3</sub>	
Lincoln 790	12.4	8.9	16.2	2.0	40.4	8.2	0.1	11.9	—	
AS 73	22.6	16.1	21.9	2.1	18.9	9.9	2.7	5.3	0.3	

inputs resulting in cooling rates from 100°C/s to not less than 8°C/s. This is a normal result for low carbon pipeline steel grades.

## 6.2 - Laboratory Welding

Under conditions similar to pipe production, the submerged arc welding process has been used to evaluate suitable wire/flux compositions. For the two-wire process a heat input of 21.6 kJ/cm in the outer position and 19.5 kJ/cm in the inner position was applied. An alumina basic flux (Lincoln 790) was tested with four different wire compositions having various amounts of Mn, Mo, Ti and B. The chemical compositions of the welding consumables are given in Table 4.

Chemical composition of the weld metal shows that independent of the wire composition a niobium content of about 0.09% has been picked up from the base plate by dilution.

Impact toughness properties of the weldment, which are of main interest, are given in Figs. 23 and 24. Only wire S3 (carbon manganese composition) shows relatively poor weld metal toughness while the best results have been obtained with Ti-Mo-B alloyed wires. Toughness in the heat-affected-zone in all weldments is similar to the properties of the base plate, even in the least tough position which is 1 mm from the fusion line.

## 6.3 - Properties of Pipe Welds

### 6.3.1 - Spiral Pipe

The above described two-wire SAW process has been applied to produce spiral pipe. The mechanical properties of the pipe material tested in the transverse direction of the pipe, which corresponds to a direction approximately 20 degrees from rolling direction, are suitable for grade X 75 pipe (Table 5).

Table 5 - Mechanical Properties of Produced Pipes

Specimen No	Pipe	R <sub>p0.2</sub> N/mm <sup>2</sup>	R <sub>m</sub> N/mm <sup>2</sup>	A <sub>1</sub> %	A <sub>180</sub> J	50% CVN- FATT °C	85% BDWT- FATT °C	
B 29	Spiral Pipe 56 inch X 15.9 mm	540	630	26	200	-90	-60	
B 33	U-O-Pipe 56 inch X 17.5 mm	483	584	26	78	-85	-55	
B 35	U-O-Pipe 40 inch X 15.0 mm	A	491	603	34	90	-80	-45
B 36		B	520	661	28	65	-65	-35
B 37		C	516	641	32	65	-65	-35

Again, the best weldment results were obtained with the S2 Ti-Mo-B wire and Lincoln 790 flux. The chemical composition of the weld metal shows a niobium pick-up of 0.09%. The tensile properties of the weld metal ( $R_e = 580 \text{ N/mm}^2$ ,  $R_m = 655 \text{ N/mm}^2$ ) adequately match those of the base material. Toughness in the weldment is also excellent. Fig. 25. The very homogeneous microstructure containing no pro-eutectoid ferrite plus the low hardness of the weld metal and HAZ are other important features. Fig. 26.

### 6.3.2 - U-O-Pipe

Three 40 inch diameter U-O-pipes have been produced from 15 mm plates, using a three-wire SAW process and a heat input of 28.8 kJ/cm. All pipes showed excellent X 70 properties (Table 5). Welding of these pipes was carried out with a wire similar to S2 Ti-Mo and a fused, boron containing amphoteric flux. Weld metal showed a tensile strength of approximately 900 N/mm<sup>2</sup>. Maximum hardness was 251 HV10. Microstructure and toughness are similar to those for spiral pipe production, Fig 27.

From one 17.5 mm thick plate, a 56 inch diameter X 70 pipe has been produced (Table 5). SAW was carried out with a heat input of 30.8 kJ/cm. However, unlike the other results, the least tough position was in the weld metal, Fig 28, due to the application of inappropriate welding consumables. These did not match the overall steel composition and were not capable of producing acicular weld metal microstructures in the presence of high niobium dilution. However, all the other properties, including HAZ toughness, meet typical X 70 requirements.

### 6.3.3 - Girth Welding

Manual metal arc welding has been carried out on the spiral pipe using cellulosic electrodes Cel 80. Heat input for root welding and hot pass was about 15 kJ/cm and about 20 kJ/cm for most of the filler and cap passes.

Microstructure (no martensite), hardness distribution and toughness properties are shown in Figs. 29 and 30. Tensile properties of the weld metal ( $R_e = 580 \text{ N/mm}^2$ ,  $R_m = 632 \text{ N/mm}^2$ ) are similar to those of the base material.

Longitudinal Pipe B (see Table 5) has been welded using the CRC-Crose automatic welding process with CO<sub>2</sub> as the shielding gas. The weld consisted of a root and five passes using a K-Nova wire. Heat input in this process was about 3 kJ/cm for the root pass and approximately 11 kJ/cm for the filler passes. Cross joint tensile tests invariably ruptured in the base metal. COD tests at 0°C showed mean values of 0.170 mm in the weld metal and 0.242 mm in the HAZ. Test results from the automatic welding trials are shown in Table 6 and the values obtained can be considered excellent when compared to other examples of X 65/X 70 automatic weldments.

The microstructures were again very homogeneous and showed an even finer austenite grain size in the HAZ as compared to other weldments of conventional X 65/X 70. Hardness distribution is shown in Fig. 31.

## 7 - Summary and Conclusions

Full-scale production of plate, strip and pipe has been carried out with a newly designed steel composition of 0.07-0.08% C, 0.35-0.45% Si; 1.50-1.60% Mn, 0.45-0.55% Ni and 0.14-0.17% Nb using different rolling conditions (variations in slab thickness, soaking temperature and time-temperature-deformation schedule) for final products in the thickness range from 13.5 to 50 mm.

The following metallurgical results have been obtained:

- the addition of about 0.50% nickel to a niobium-microalloyed low carbon manganese steel lowers the transformation temperature so that even finishing temperatures of 710°C are fully in the austenite region;
- the applied niobium content either remained undissolved during soaking or was precipitated predominantly (80 to 95%) in the austenite during rolling. This was particularly true when a high degree of pre-rolling was applied to thicker slabs or a high degree of final deformation was applied in the temperature range 900 to 800°C. Lower or higher finish rolling temperatures, outside the 800-900°C range, as well as higher soaking temperatures, resulted in a somewhat smaller amount of coarse precipitates in the size range of 200 to 2000 Å;
- the niobium fraction which was not precipitated in the above mentioned temperature range, precipitated almost completely either by stress-induced processes in the metastable austenite region, during  $\gamma - \alpha$  transformation or in the ferrite region. The precipitates had a resulting particle size which makes a remarkable contribution to strength increase;

Table 6 - Mechanical Properties of Actual CRC Weldment

Test Position	Weld Metal				HAZ			Cross Joint Tensile Rm N/mm <sup>2</sup>			
	Rp <sub>0.2</sub> N/mm <sup>2</sup>	Rm N/mm <sup>2</sup>	Charpy-V at 0°C		COD-TTN at 0°C						
			J	% Shear	mm						
12 o'clock	637	756	65	58	0.212	0.220	0.235	0.193	0.167	0.195	614
3 o'clock	639	756	48	48	0.069	0.171	0.114	0.332	0.244	0.297	612
6 o'clock	614	726	—	—	0.204	0.149	0.151	0.242	0.164	0.307	610
9 o'clock	629	733	—	—	0.202	0.153	0.155	0.236	0.251	0.277	622

- independent of the rolling conditions applied, the free nitrogen content of all rolled products was very low, thus contributing to the good toughness obtained;
- another contribution to the low FATT was from the fine ferrite grain size of the steel. The actual grain size was a function of the final total deformation below the recrystallization temperature, the plate thickness, and cooling rate after finish rolling;
- the transformation behaviour of this steel grade under welding conditions is characterized by a wide zone of bainitic microstructure. This guarantees excellent heat-affected-zone properties for the welding processes usually applied in pipe production. These include submerged arc welding and manual and automatic field welding. The excellent properties result from the lack of martensite islands and proeutectoid ferrite.

The mechanical properties obtained with this steel composition result in X 65 properties with excellent toughness for 18 mm plate rolled with a finish rolling temperature of approximately 820°C. Compared with other pipe line steel grades, these are rather light rolling conditions. A lower finishing temperature or accelerated cooling lead to higher tensile properties, again with excellent toughness. For example, finish rolling at 720°C or strip production results in X 75/X 80 strength properties with a BDWTT-FATT of -50°C. Only finish rolling temperature above 900°C, combined with a high plate thickness, result in inadequate transition temperature.

Excellent toughness properties, reasonable maximum hardness values and no cold cracking were features of the heat-affected-zone for all welding processes investigated. In the submerged arc welding process a certain amount of niobium is picked up by dilution of base plate into the weld metal. As a result, wires of selected chemical composition have to be used which result in an appropriate microstructure after transformation (e.g. Ti-Mo-B alloyed material). When using such a wire composition, excellent weld metal toughness was obtained.

The results of this investigation show that the simple addition of approximately 0.50% nickel and 0.15% niobium to a low-carbon-manganese steel is an alternative route for producing X 65 to X 75 pipe steel with excellent toughness and weldability. In the production of these steel grades comparatively light rolling conditions can be applied which result in various technical and production advantages. By means of better knowledge of the metallurgy of this steel grade and optimization of chemical composition and rolling schedules it is likely that properties of Ni-Nb alloyed HSLA steels may be further improved.

## LITERATURE

- 1 - K. Lorenz, W.M. Hoff, K. Hulka, K. Kaup, H. Litzke and U. Schrape, "Thermomechanical and temperature controlled rolling of plates and hot strips", *Stahl und Eisen*, 101 (1981) 593.
- 2 - H. Jesper and K. Achtelik, "Cryogenic steels", Nickel Informationsbüro, Düsseldorf, 1960.
- 3 - J.M. Gray, personal communication, Microalloying International, Houston, 1979.
- 4 - Euronorm 129/76.
- 5 - H. Baumgardt, H. de Boer and F. Heisterkamp, "Review of microalloyed structural plate metallurgy, alloying, rolling and heat treatment", International Conference Niobium'81, San Francisco, 1981. Proceedings to be published.
- 6 - K. Hulka, "Ferritic structural steels for low temperature application", *Peine Salzgitter Berichte*, 1 (1981) 11.
- 7 - T. Gladman, D. Dulieu and I. D. McIvor, "Structure property relationship in high strength microalloyed steels", *Microalloying '75*, Union Carbide Corporation, New York, 1977, p. 32.
- 8 - J.M. Chilton and M.J. Roberts, "Structure property relationship in hot-rolled low-carbon steels finished at normal hot-rolling temperatures", *Vanadium in High Strength Steel*, Vanitec, London, 1979, p. 11.
- 9 - I. Kozasu, C. Ouchi, T. Sampei and T. Okita, "Hot rolling as high temperature thermomechanical process", *Microalloying '75*, Union Carbide Corporation, New York, 1977, p. 120.
- 10 - T. De Ardo, L. Meyer and J.M. Gray, "Fundamental metallurgy of niobium in steel", International Conference Niobium'81, San Francisco, 1981. Proceedings to be published.
- 11 - F. Heisterkamp, J.M. Gray and H. Stuart, "Niobium as a toughening element in pipe steel: influence on weldment properties", *2<sup>nd</sup> Conference on Pipe Welding*, The Welding Institute, London, 1980, vol. 1, p. 307.
- 12 - G. Lütjering and E. Hornbogen, "Mechanical properties of solid solution in ferrite", *Z. Metallkunde*, (1968) 29.
- 13 - L. Meyer and H. de Boer, "HSLA plate metallurgy: alloying, normalizing, controlled rolling", *J. Metals*, 29 (1977) 17.
- 14 - M. Kretschmer and K. H. Koch, "Nitride formation in microalloyed steels — possibilities of qualitative and quantitative evaluation", *Estel Berichte*, 2 (1976) 92.
- 15 - J. Heslops and N. J. Petch, "Dislocation locking and fracture of  $\alpha$ -iron", *Philosophical Magazine*, 2 (1957) 649.
- 16 - W. B. Morrison, "The effect of grain size on the stress-strain relationship in low-carbon steel", *ASM Transactions Quarterly*, 59 (1966) 824.
- 17 - J.M. Gray, "Effect of niobium (columbium) on transformation and precipitation processes in high-strength low-alloy steels", *Heat Treatment '73*, The Metals Society, London, 1973.
- 18 - D.A. Litvinenko, I.I. Frantov, Yu. Morazov and V.I. Stolianov, "Essays of plates and of weldability of controlled rolled pipe steel", Internal Report of the Bardin Institute, Moscow, 1981.

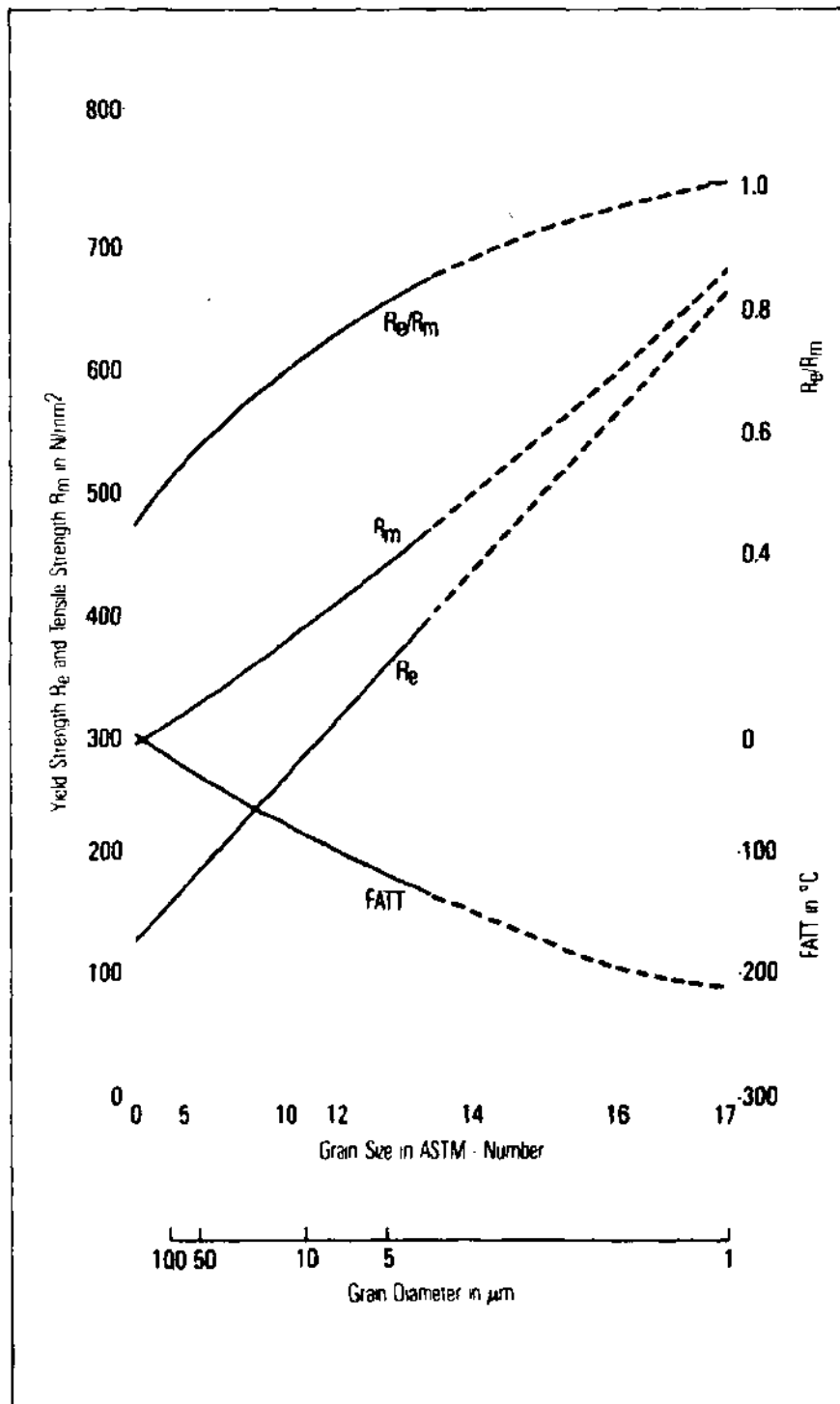


Fig. 1 — Yield point, tensile strength and transition temperature of a low carbon steel as a function of grain size.



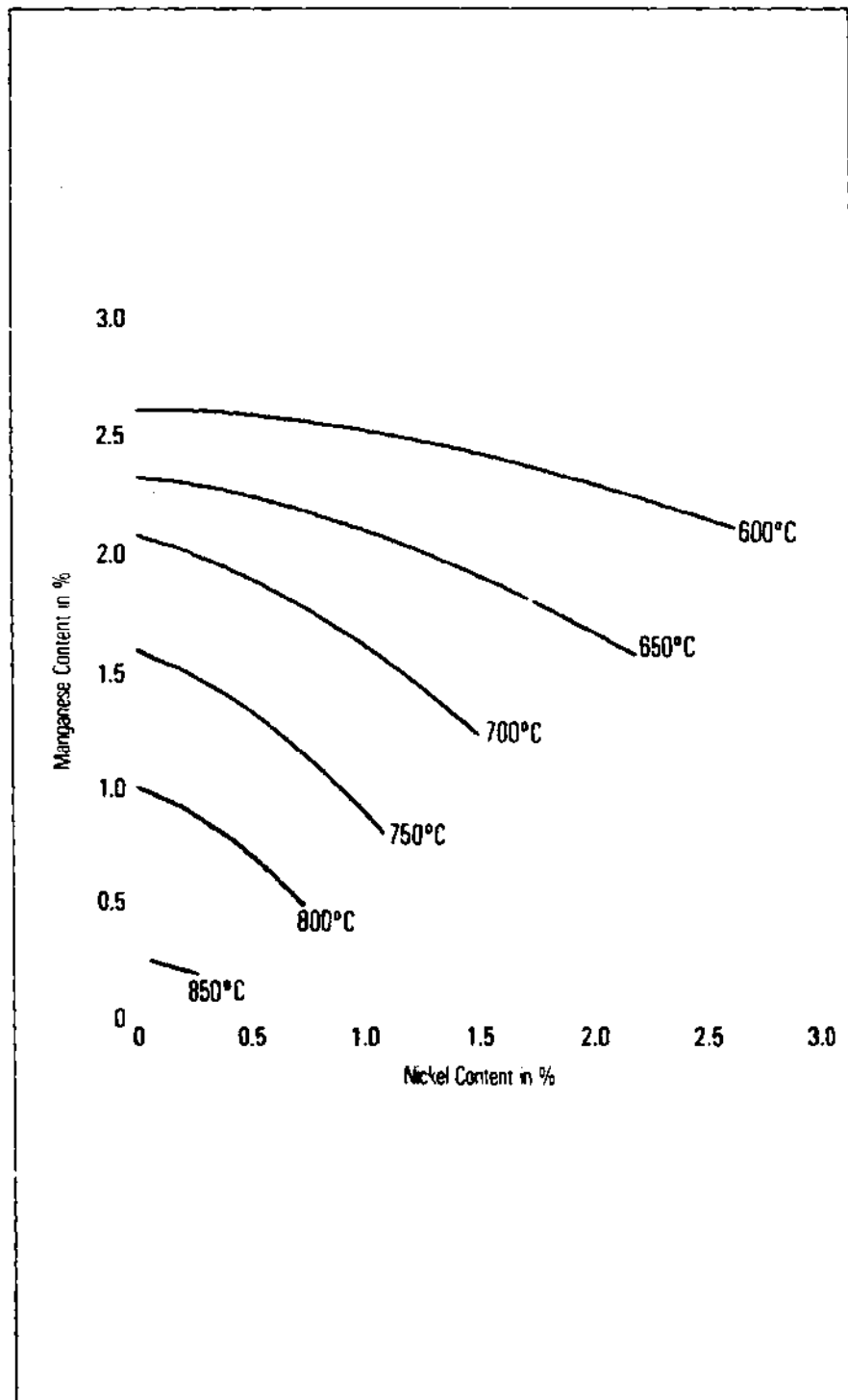


Fig. 2 — Ar<sub>3</sub> - Temperatures for 0.035% C - 0.045% Nb steels with various Ni and Mn-contents.

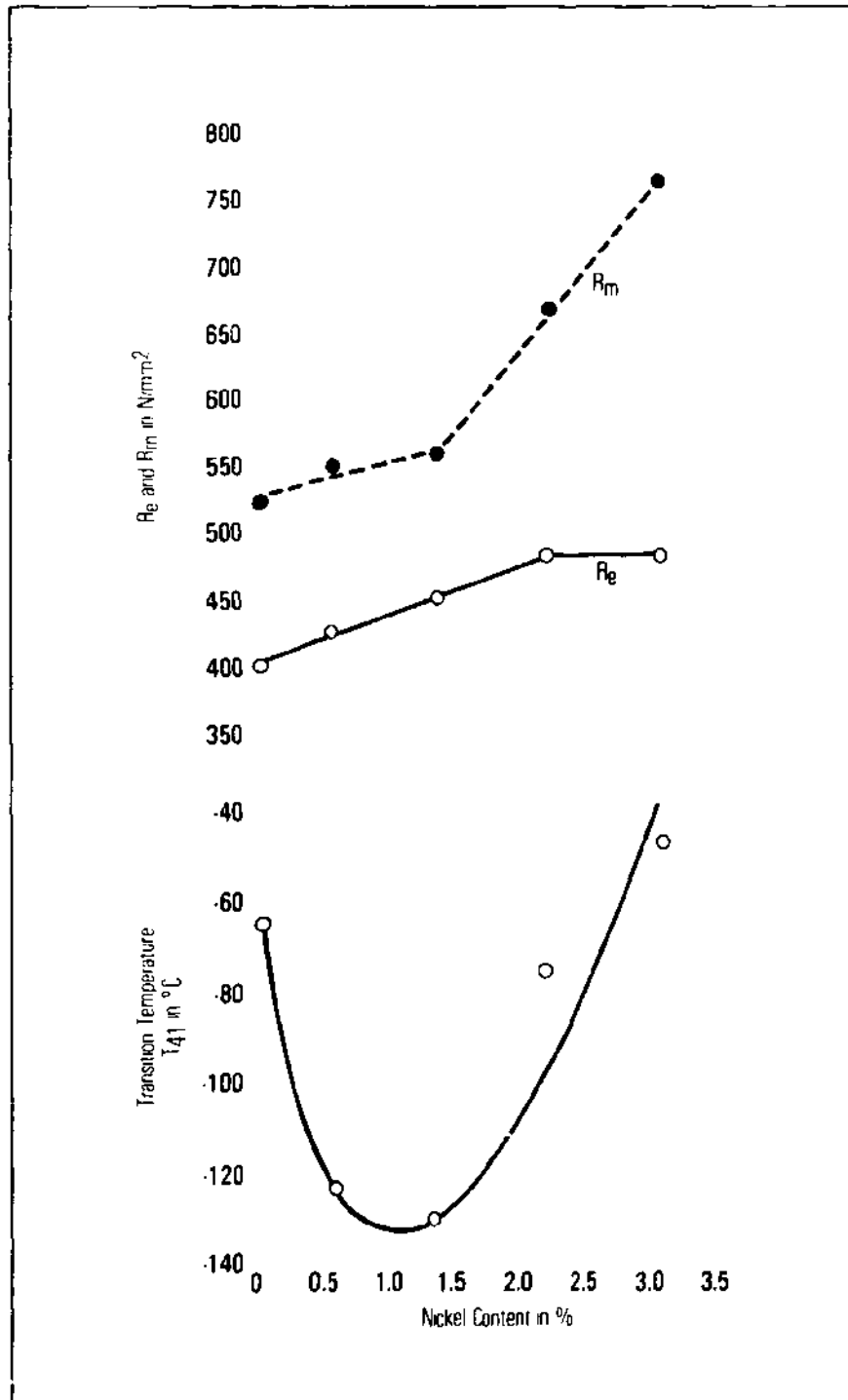


Fig. 3 — Influence of Ni content on the transverse mechanical properties of niobium microalloyed LPG steel grades. Base composition: 0.09% C, 0.31% Si, 1.46% Mn, 0.015% P, 0.013% S, 0.038% Al, 0.07% Nb.

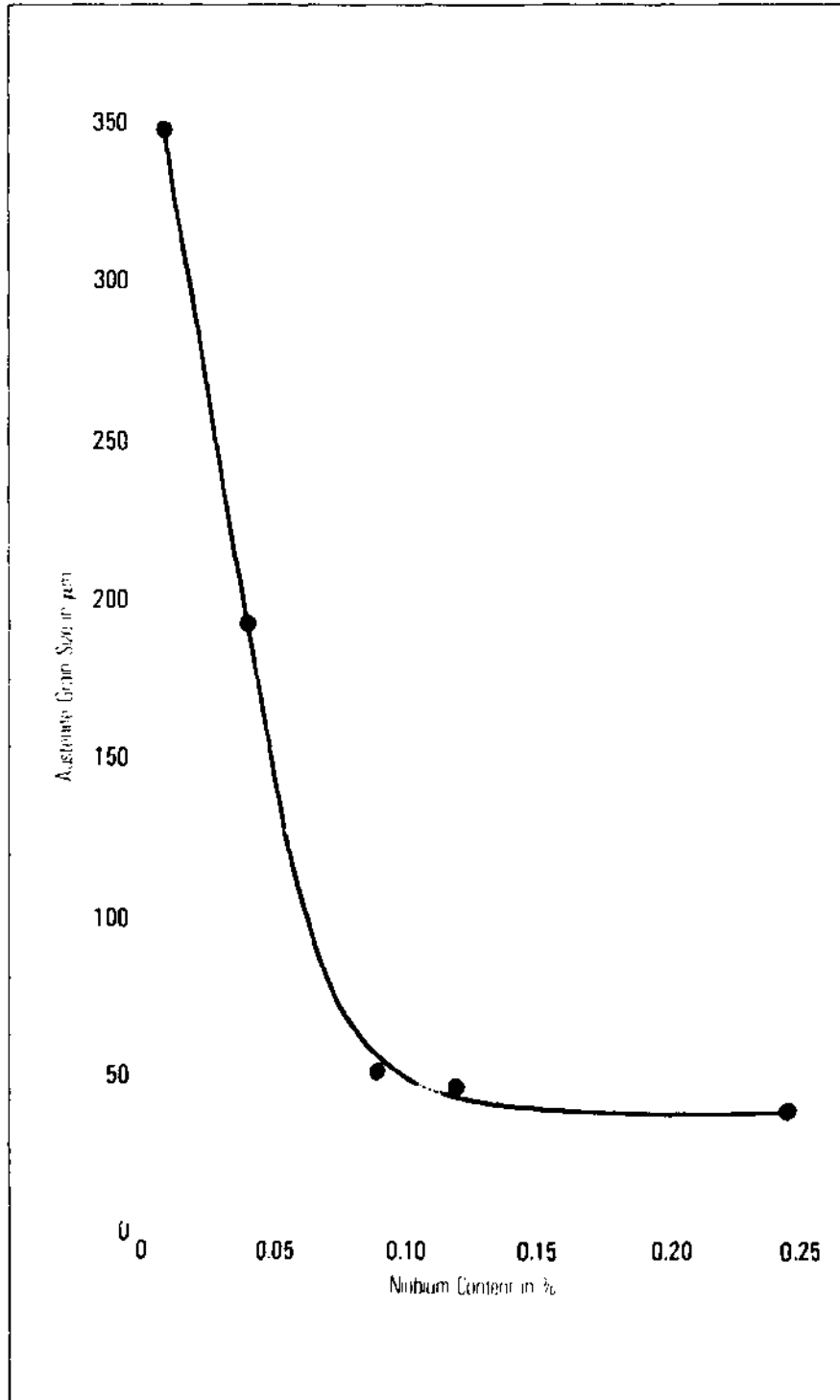


Fig. 4 — Effect of niobium content on austenite grain size at 1175°C soaking temperature.

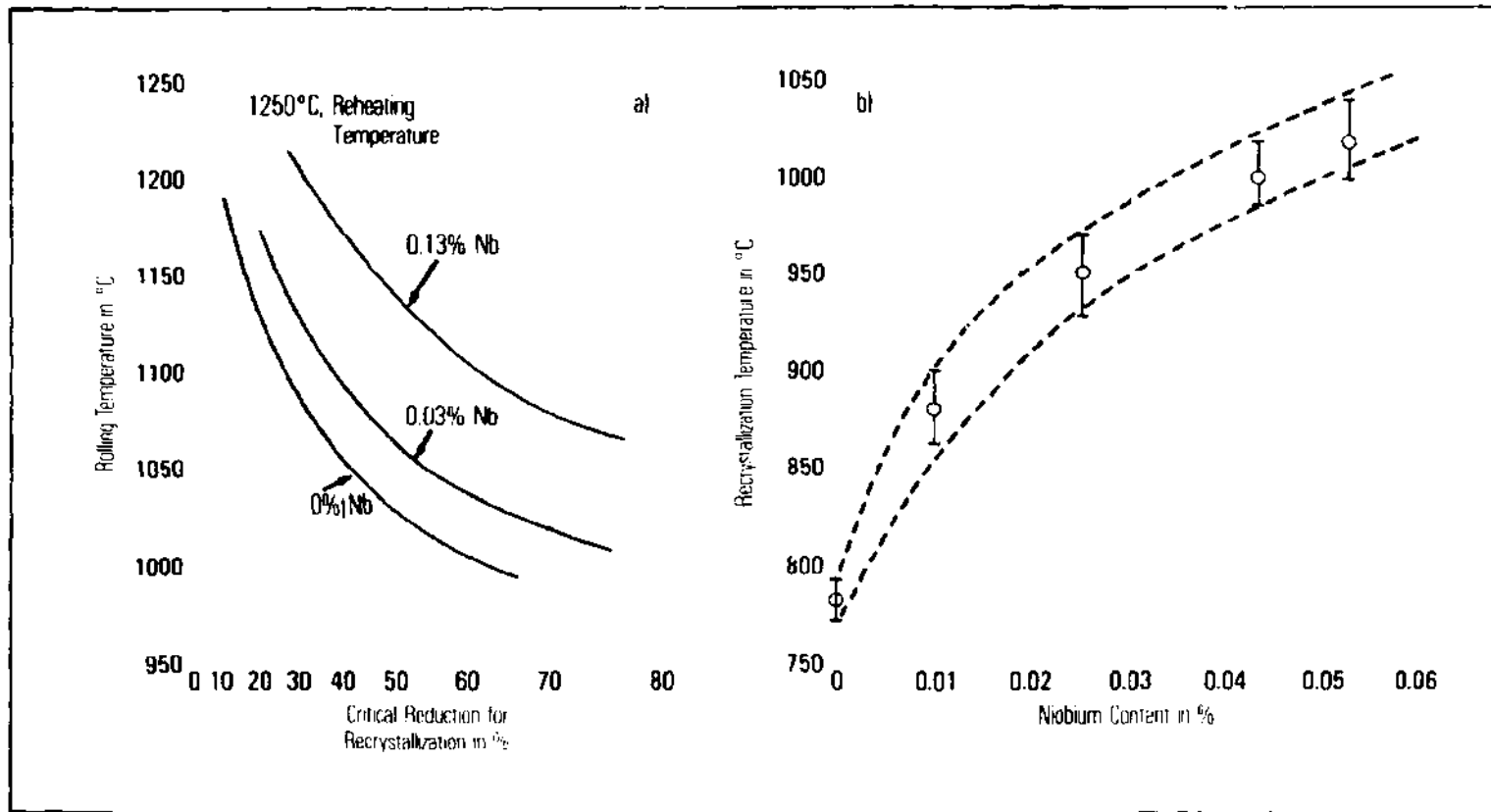


Fig. 5 — Effect of niobium on critical reduction and temperature for austenite recrystallization.

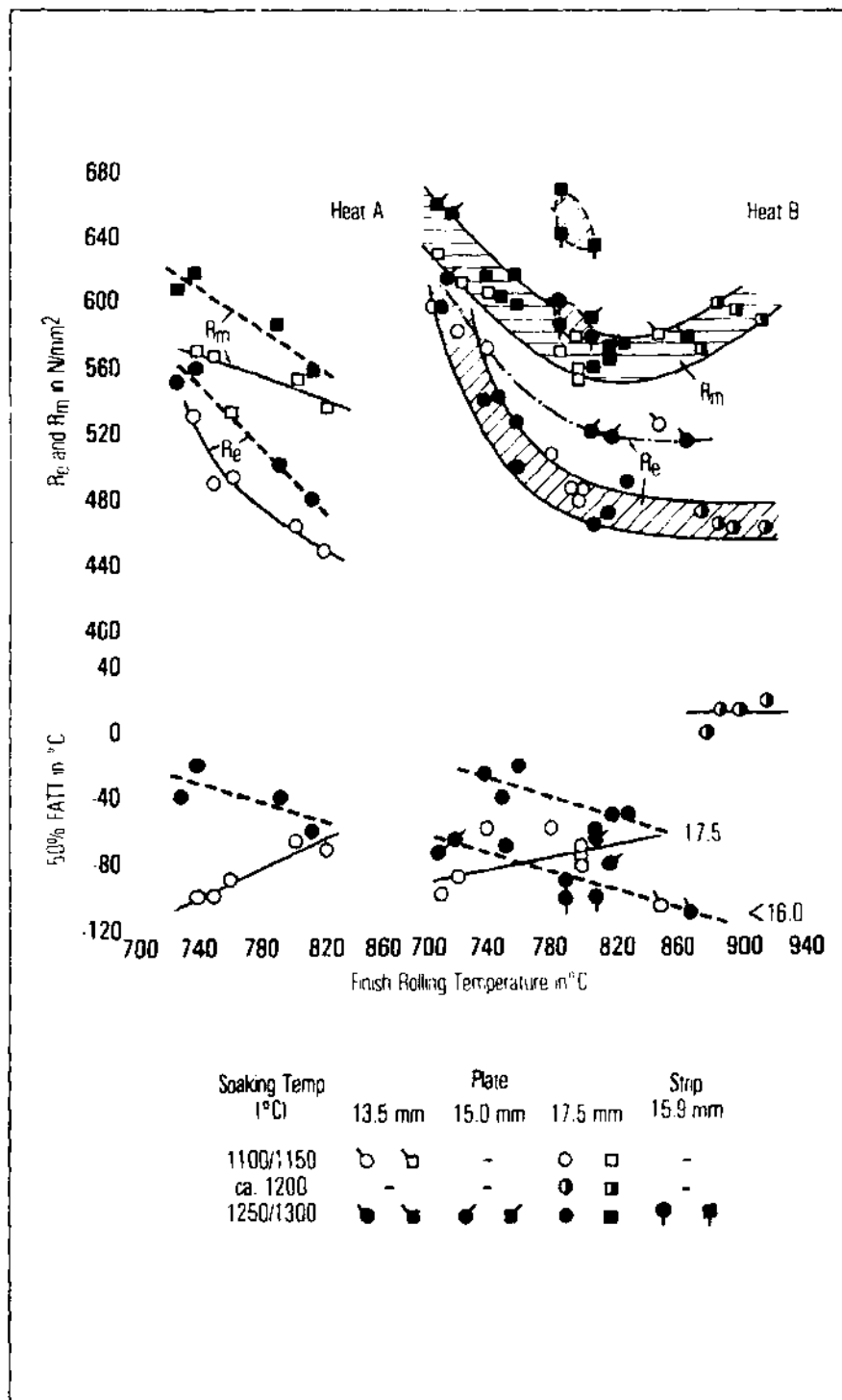


Fig. 6 — Influence of rolling conditions on the mechanical properties of plate and strip material, th.  $\leq 17.5$  mm.

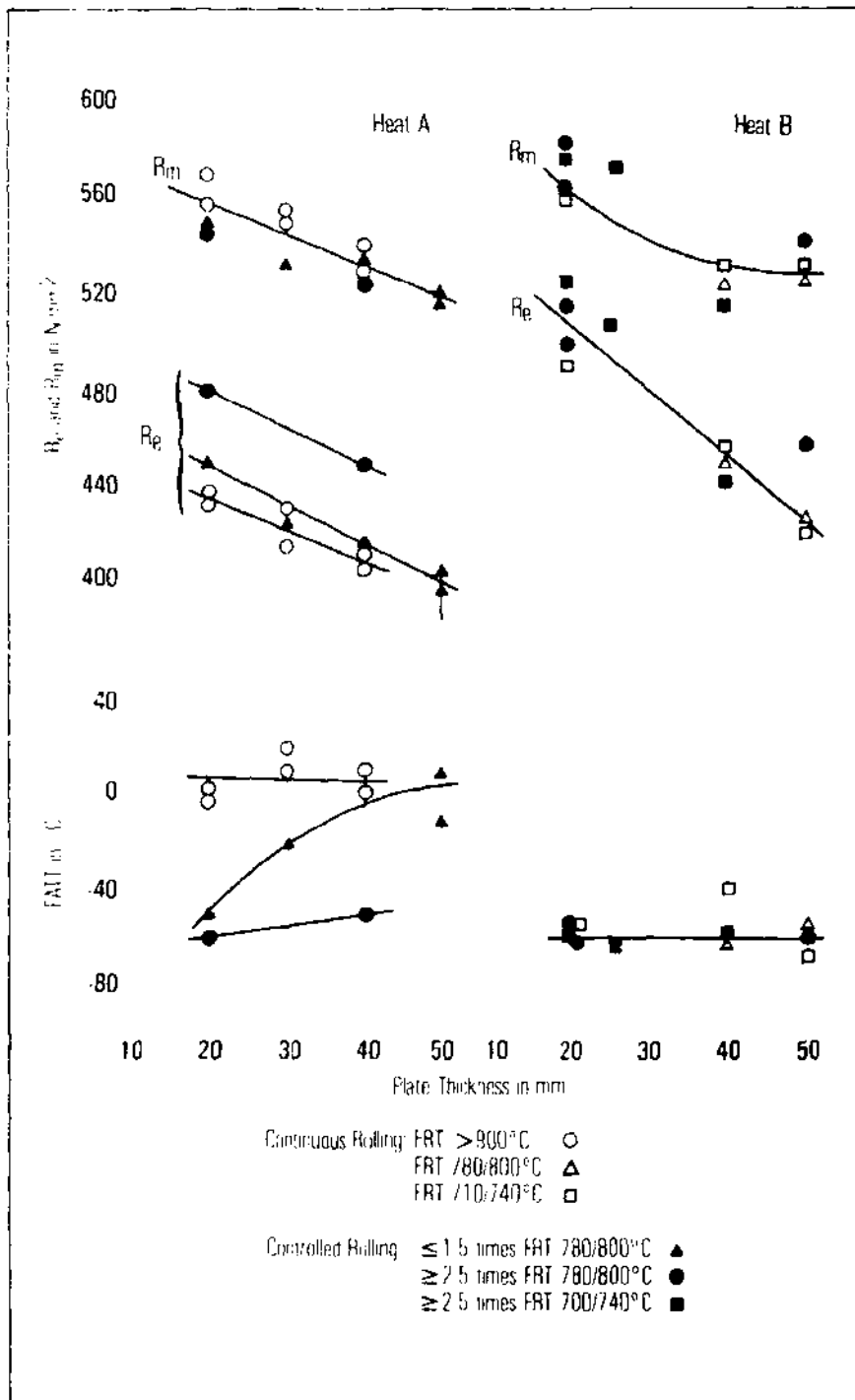


Fig. 7 — Influence of plate thickness on mechanical properties for different rolling conditions (soaking temperature  $\approx 1200^{\circ}\text{C}$ ).

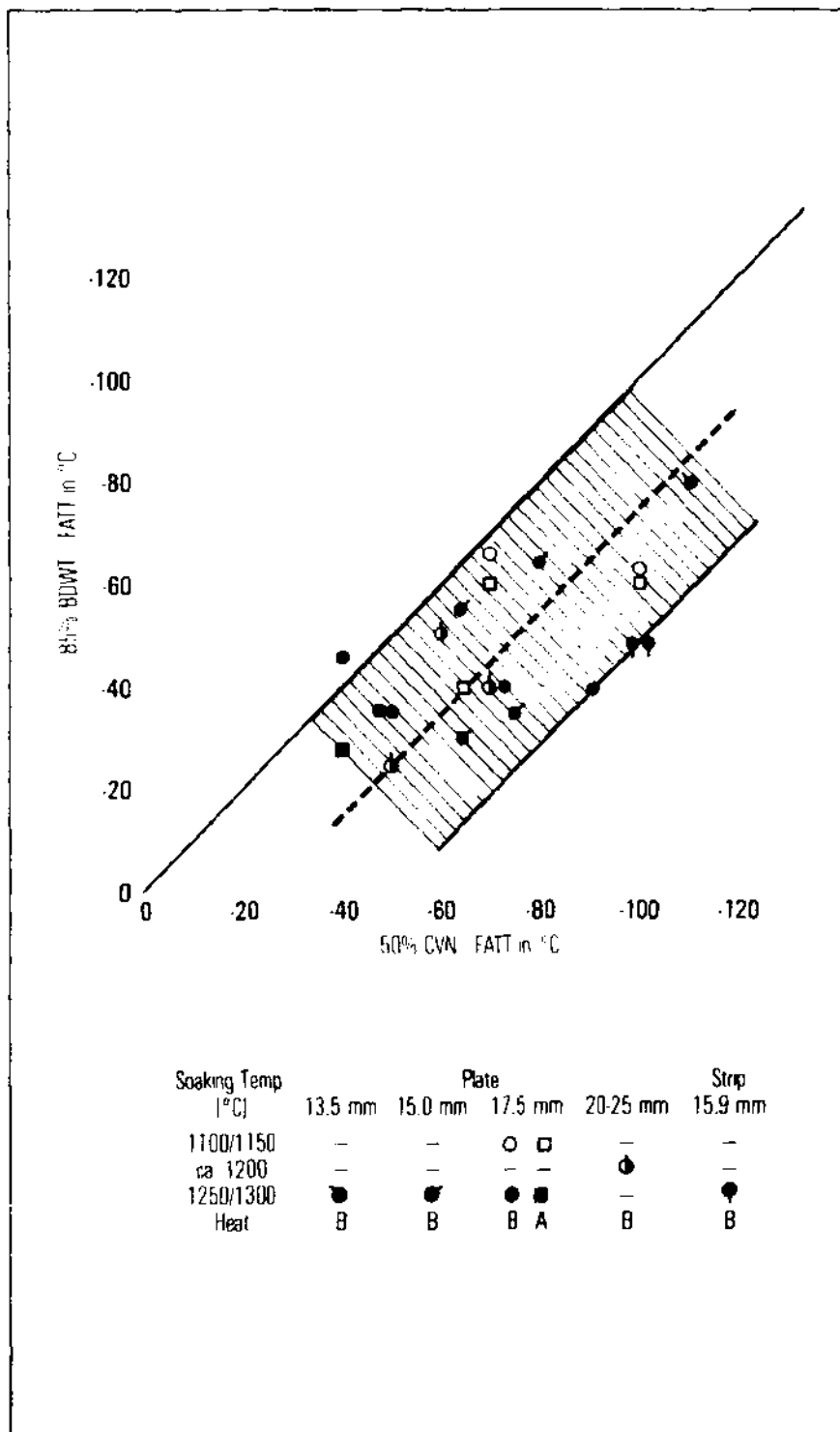


Fig. 8 — Correlation between CVN and BDWT test results.

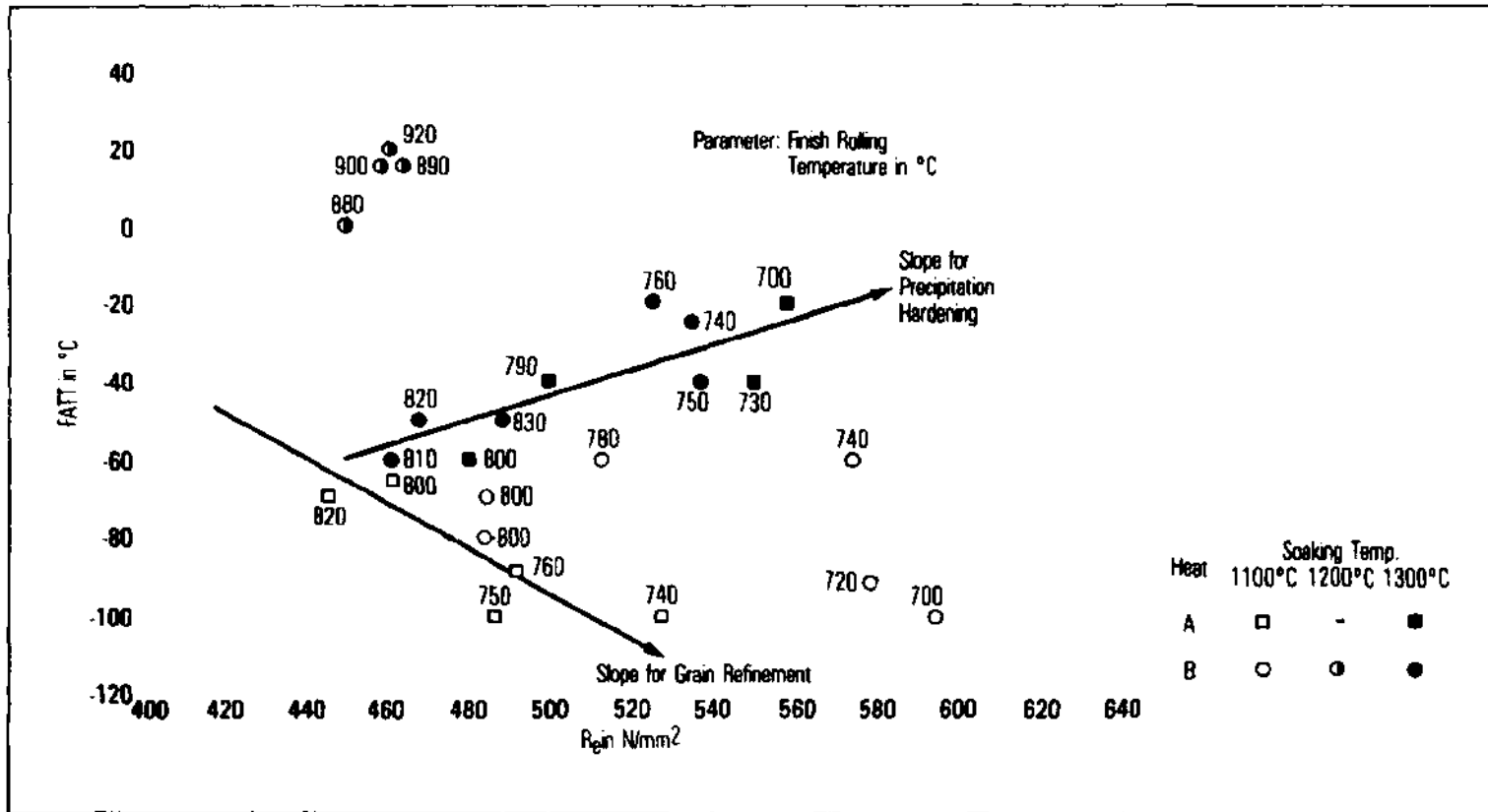


Fig. 9 — Correlation between strength, toughness, grain refinement and precipitation hardening for 17.5 mm plates.



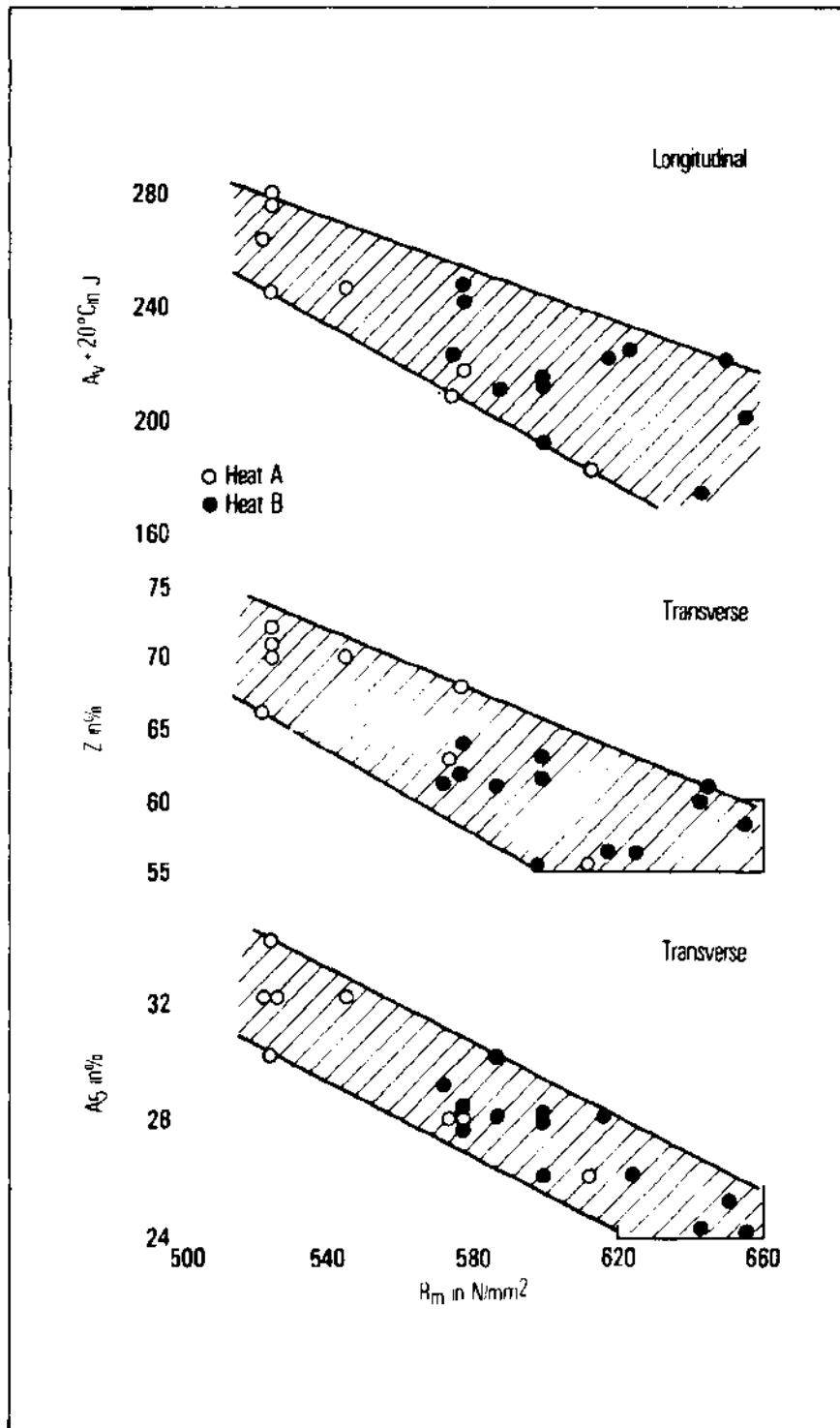


Fig. 10 — Ductility properties of NiNb plates.

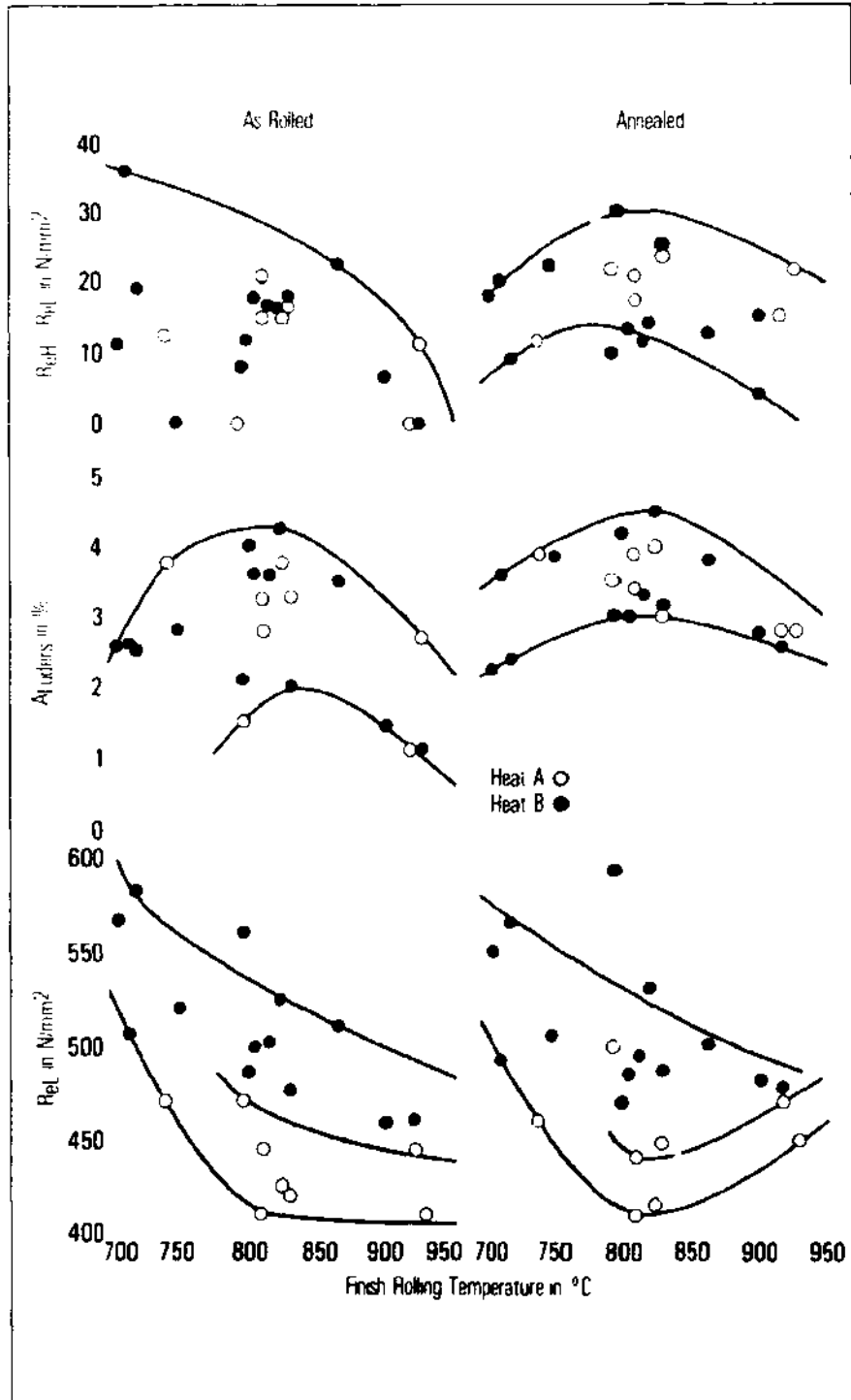


Fig. 11 — Form of yield point and influence of annealing (600°C/30 min.) (transverse).

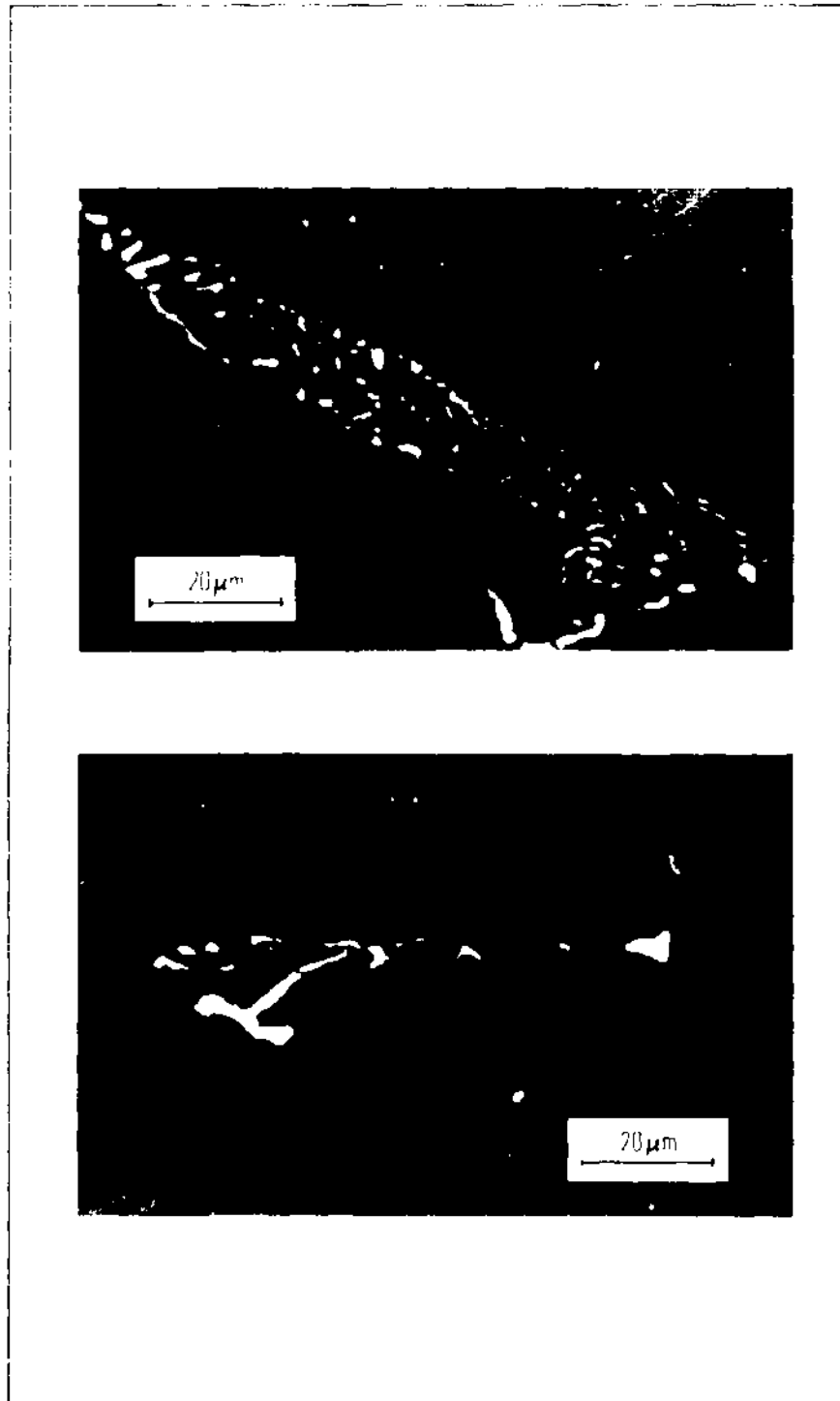


Fig. 12 — Niobium carbide inclusions in eutectic formation (ZnSe coated).

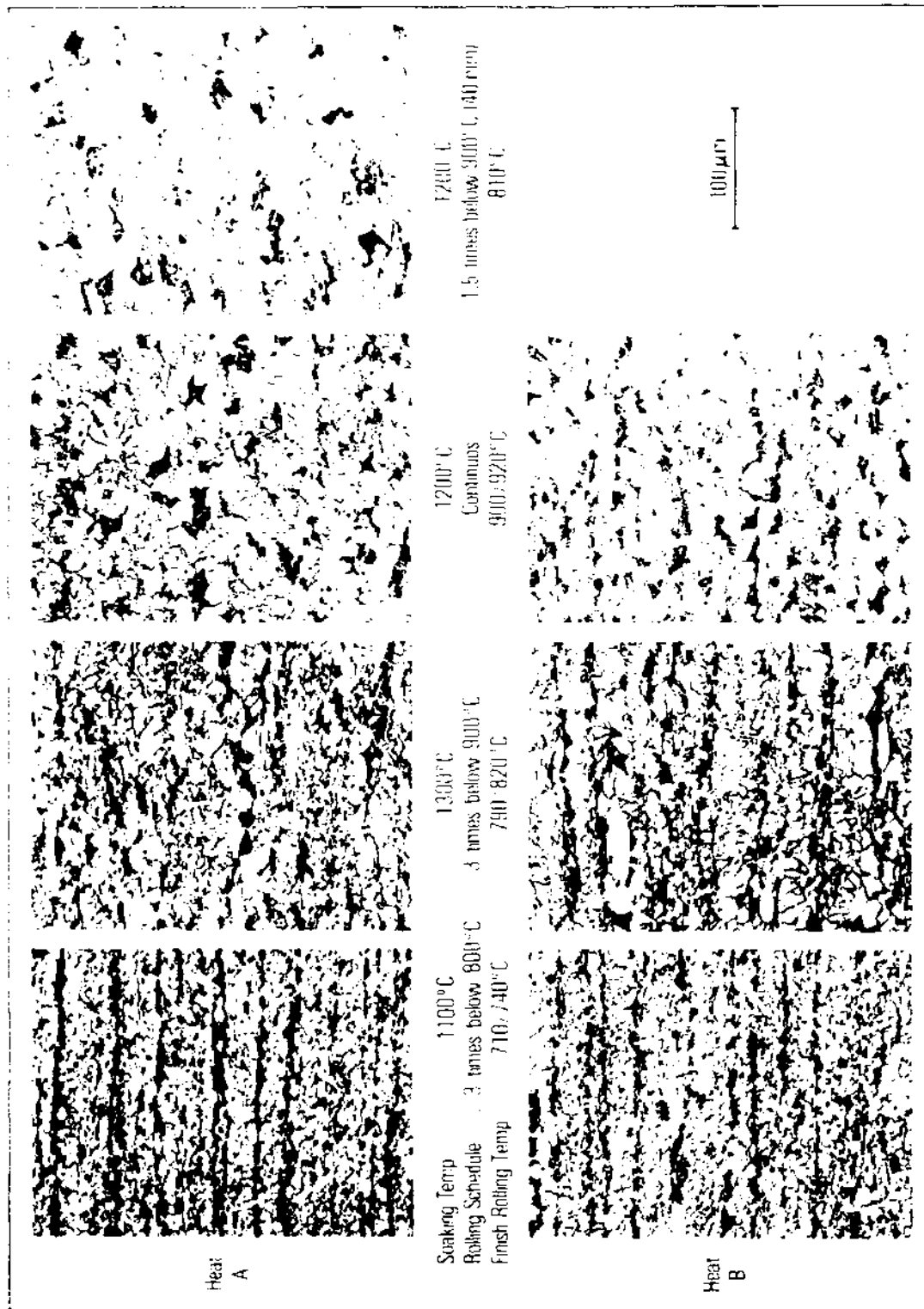


Fig. 13 — Microstructure of Ni Nb steel plates after various rolling conditions.

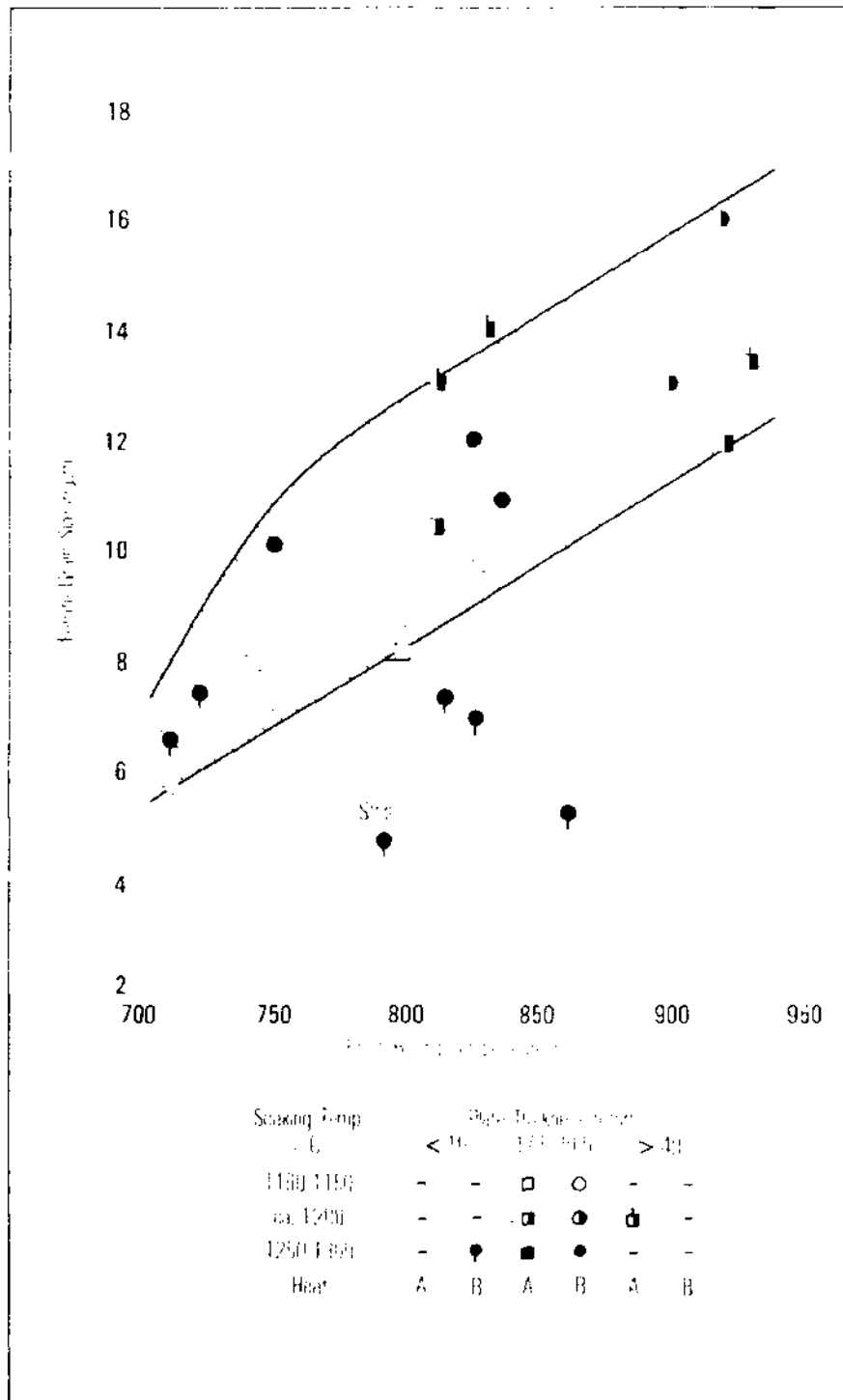


Fig. 14 — Influence of rolling conditions on the average ferrite grain size.

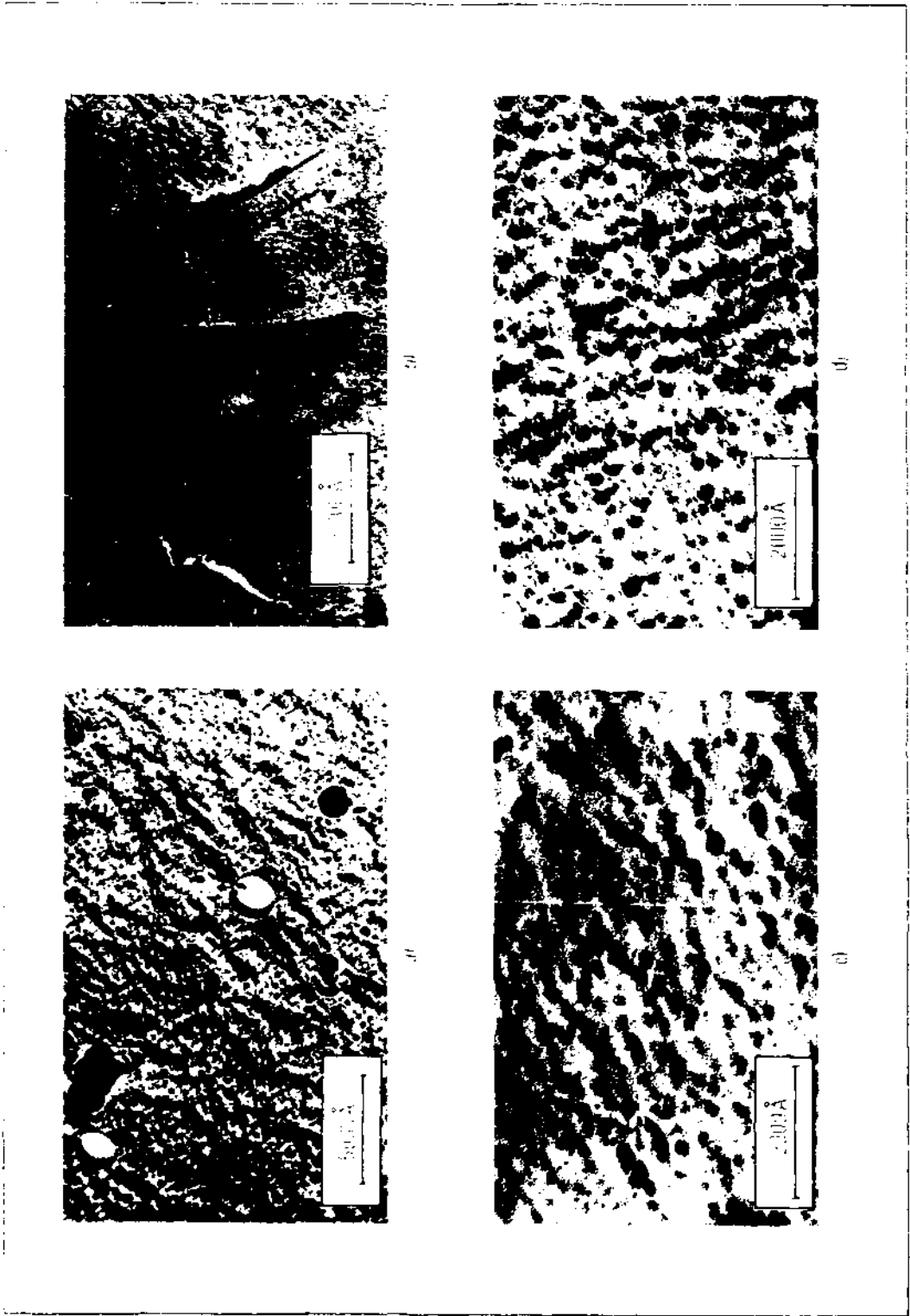


Fig. 15 — Examples for Nb (C, N) precipitates with different particle size - a) about 2000 A - b) about 200 A - c) about 20 A - d) about 40 A (transmission electron microscope, replica technique).

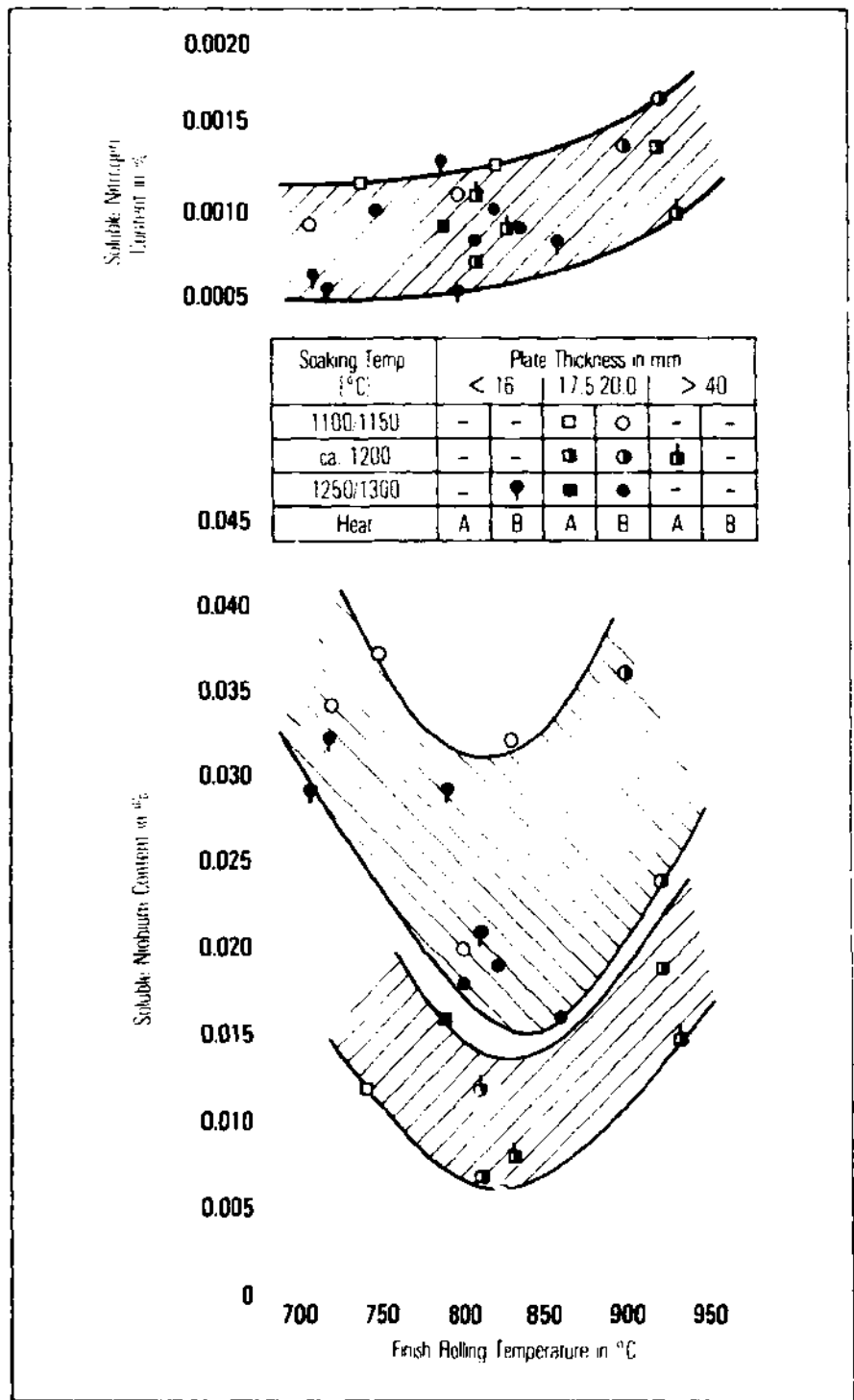


Fig. 16 — Influence of rolling conditions on soluble nitrogen and soluble niobium content.

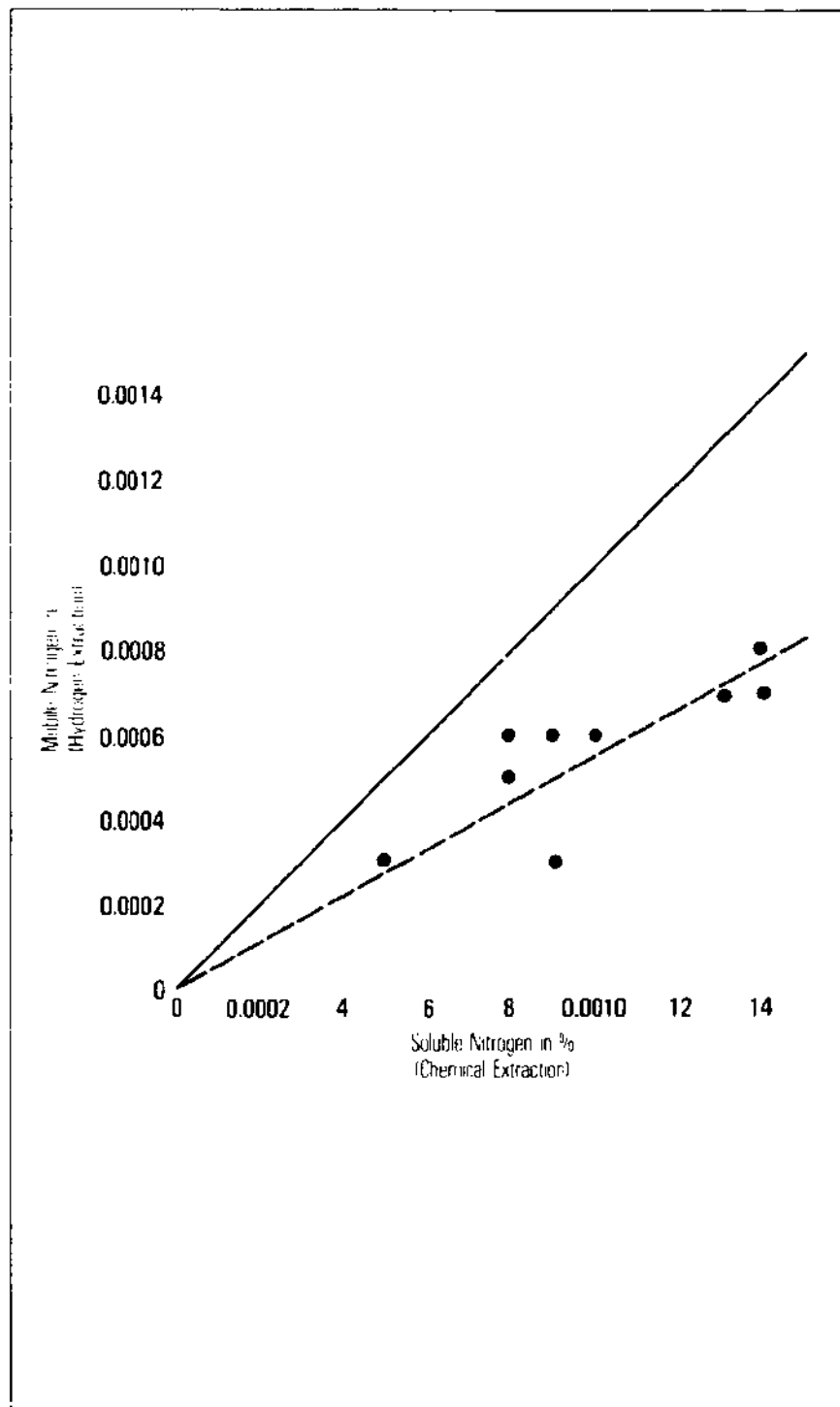


Fig. 17 — Comparison of free nitrogen content evaluated by chemical extraction and by hydrogen extraction technique.



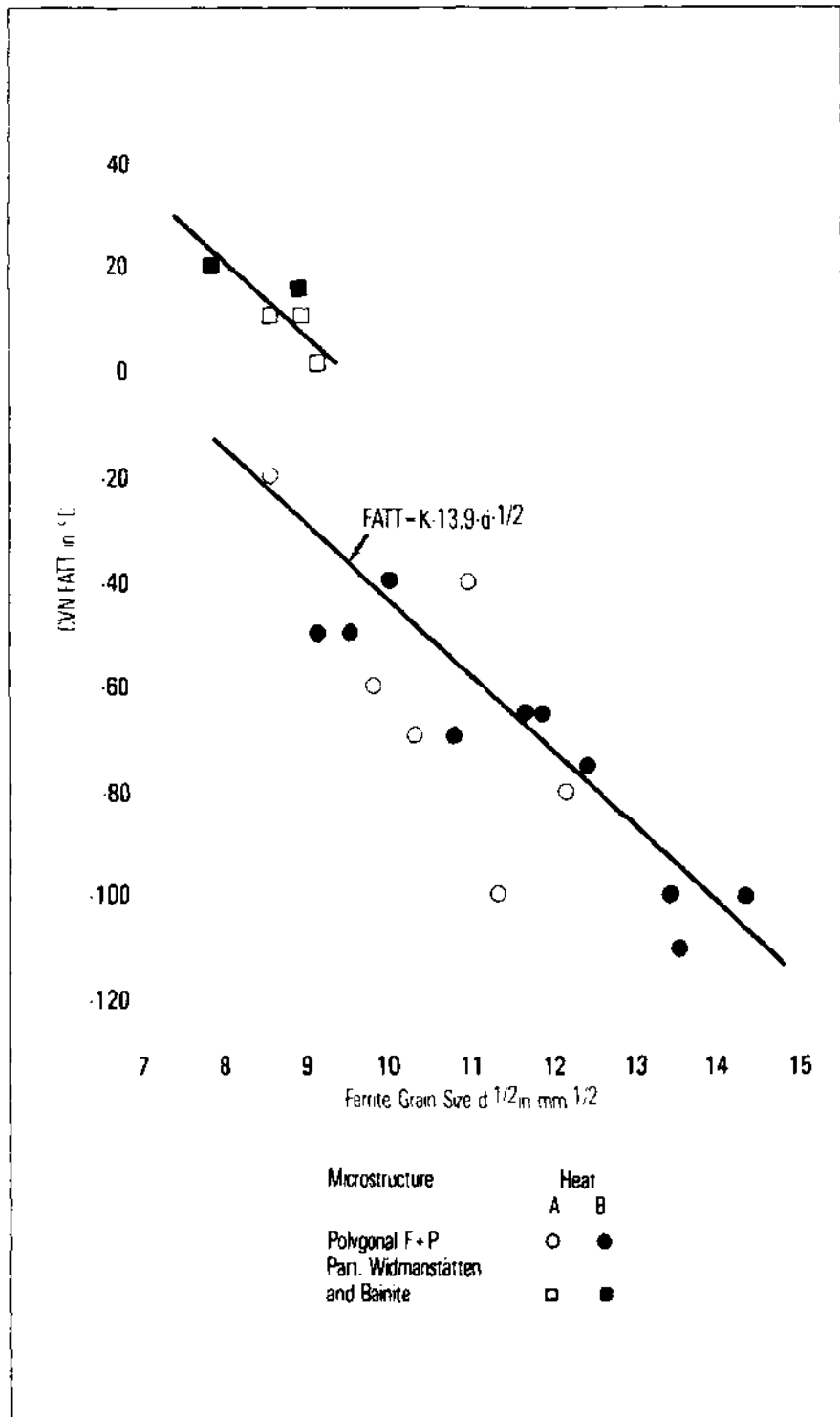


Fig. 18 — Correlation between ferrite grain size and CVN-FATT.

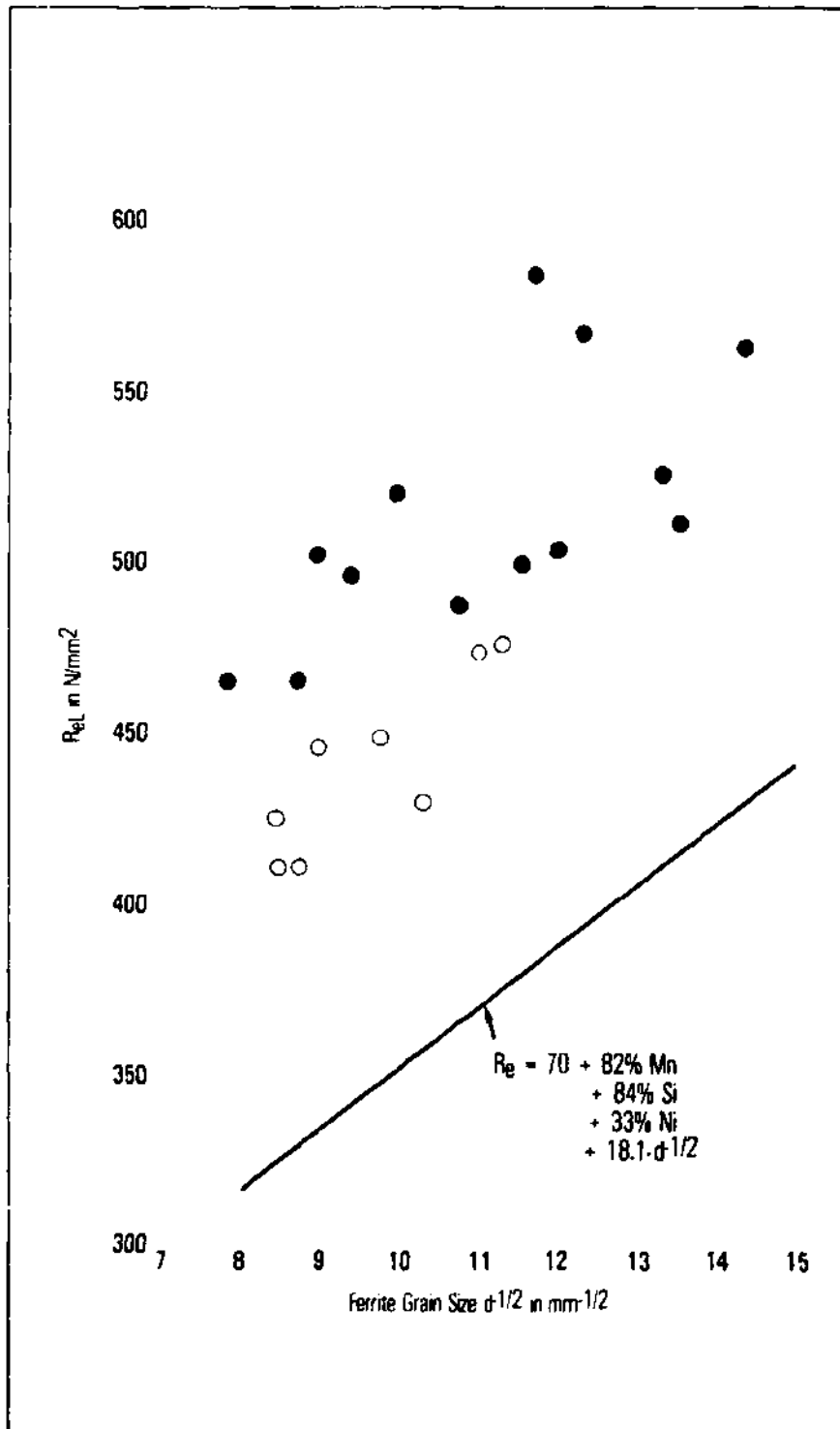


Fig. 19 — Correlation between ferrite grain size and yield strength.

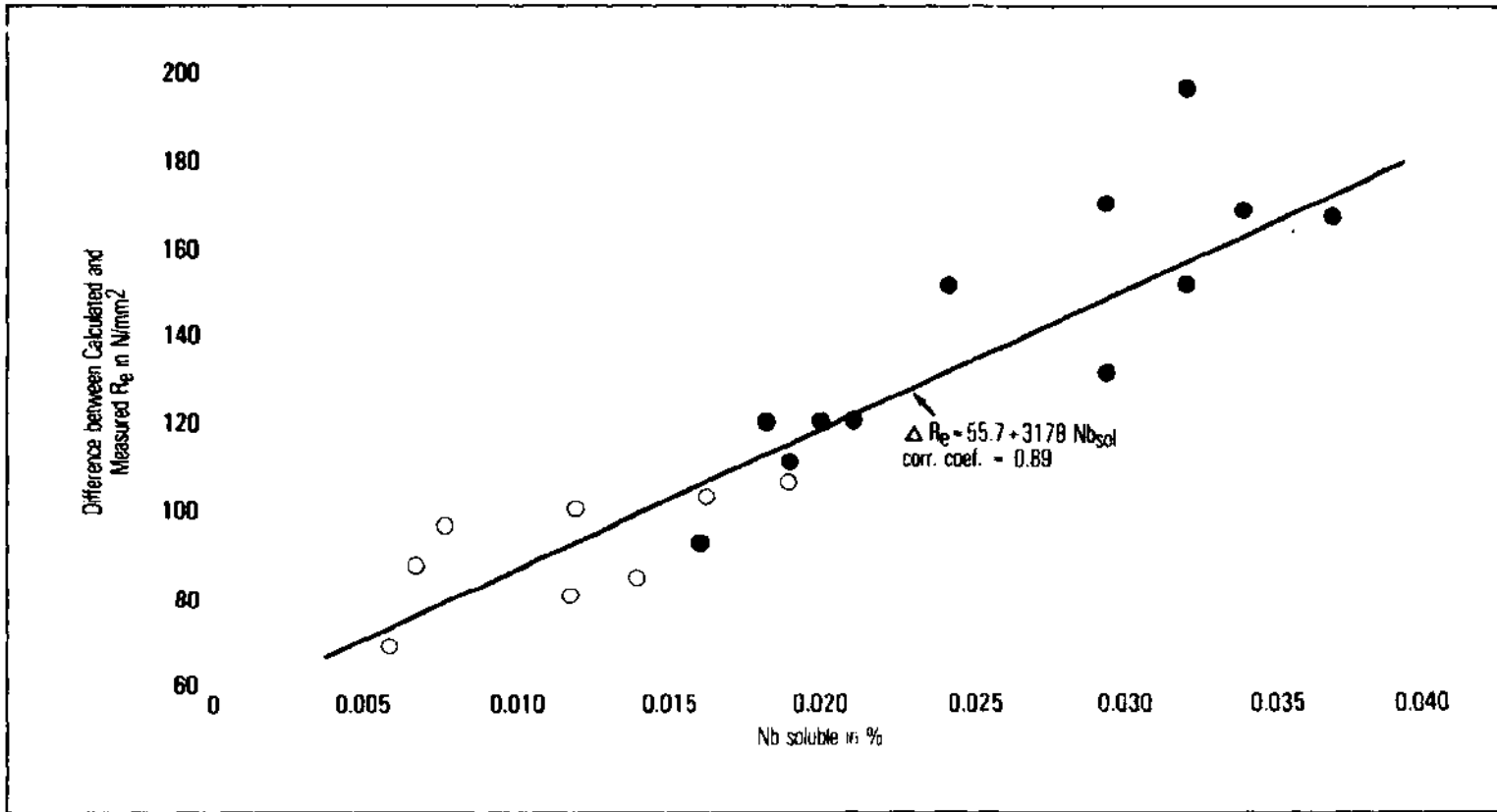


Fig. 20 — Correlation between soluble niobium content and yield strength increase.

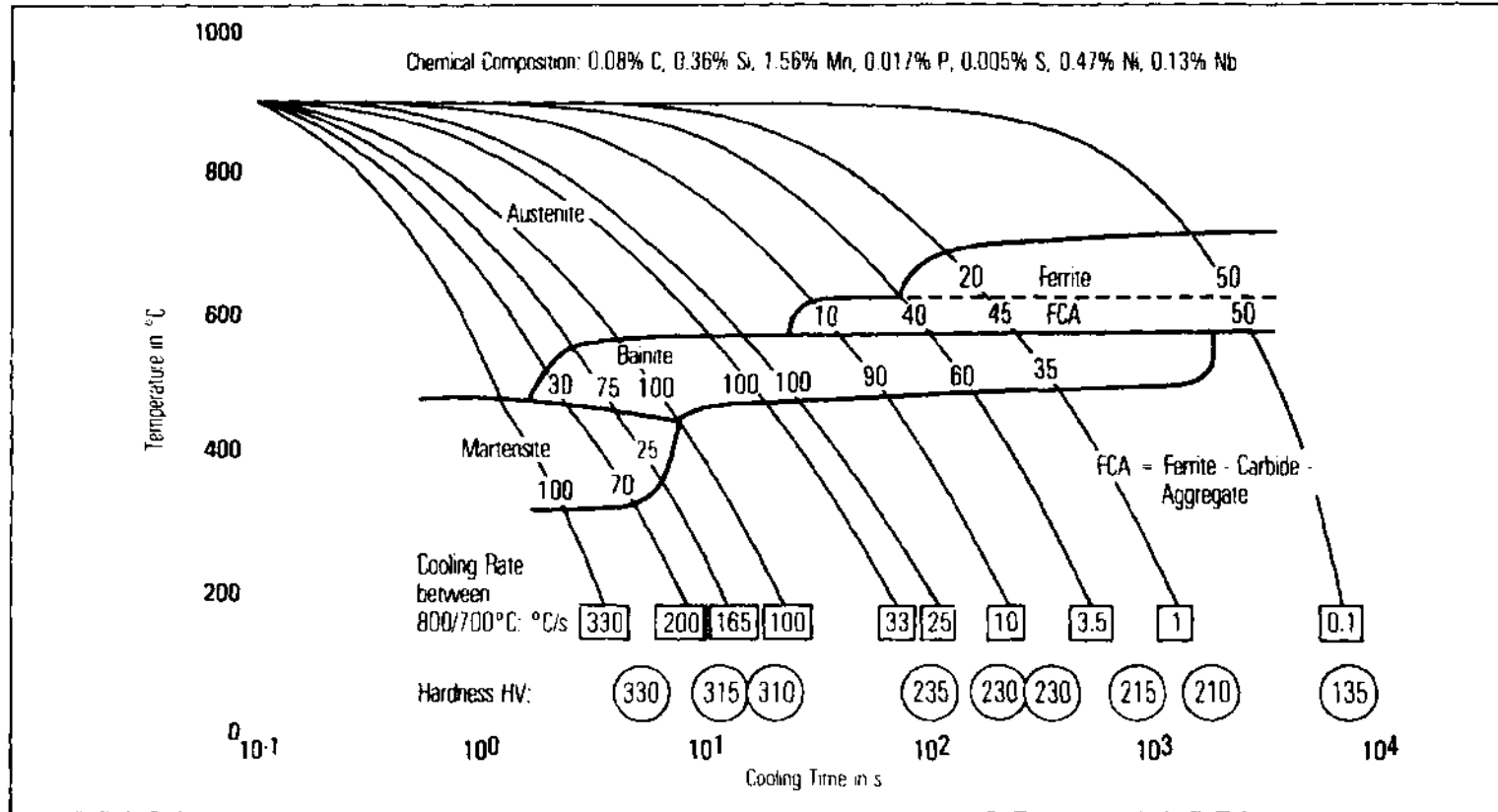


Fig. 21 — CCT - Diagram of Ni Nb steel after austenitizing at 1350°C.

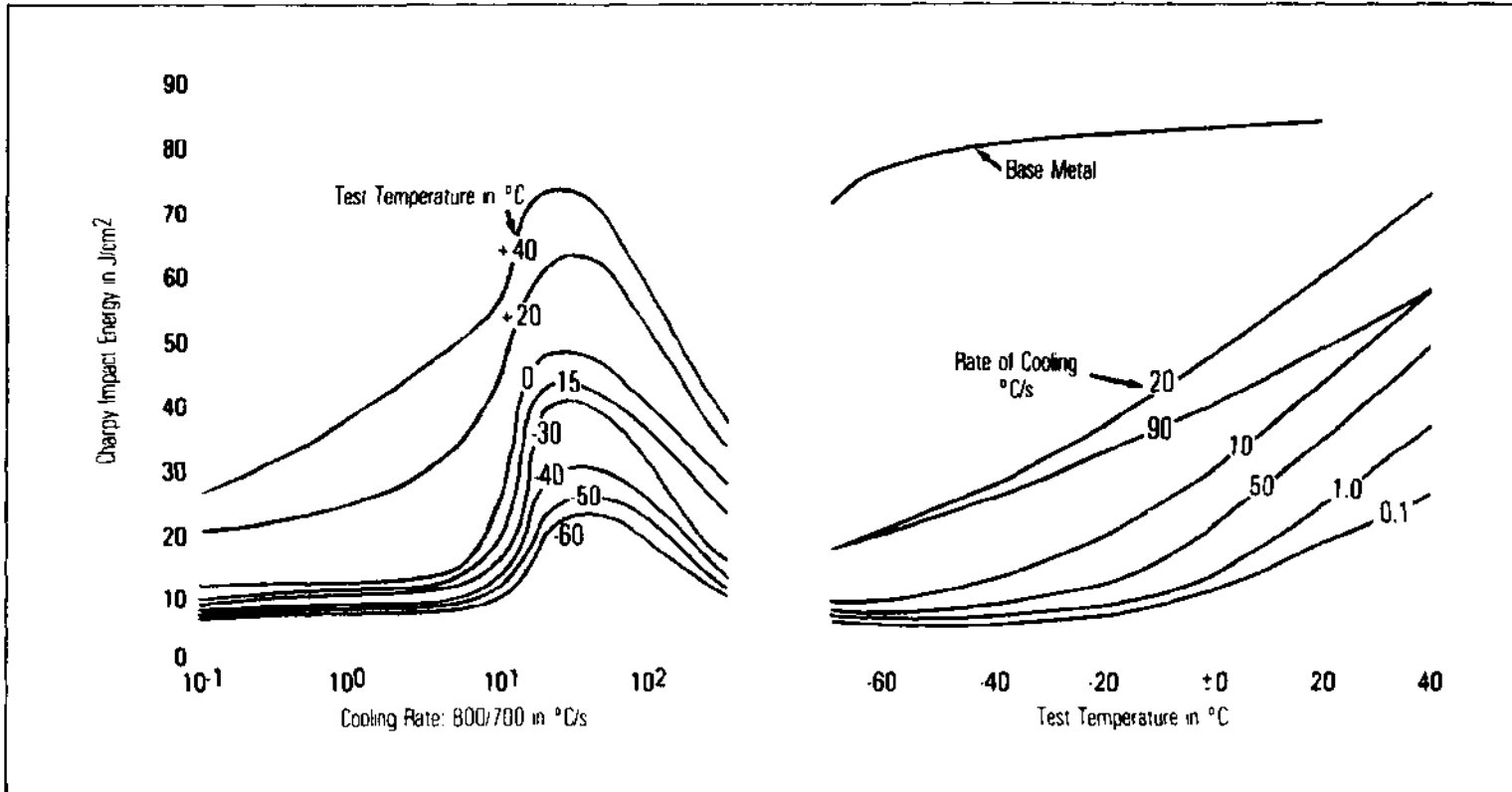


Fig. 22 — Influence of cooling rate on impact toughness of simulated heat affected zone of Ni Nb steel (peak temp.: 1350°C).

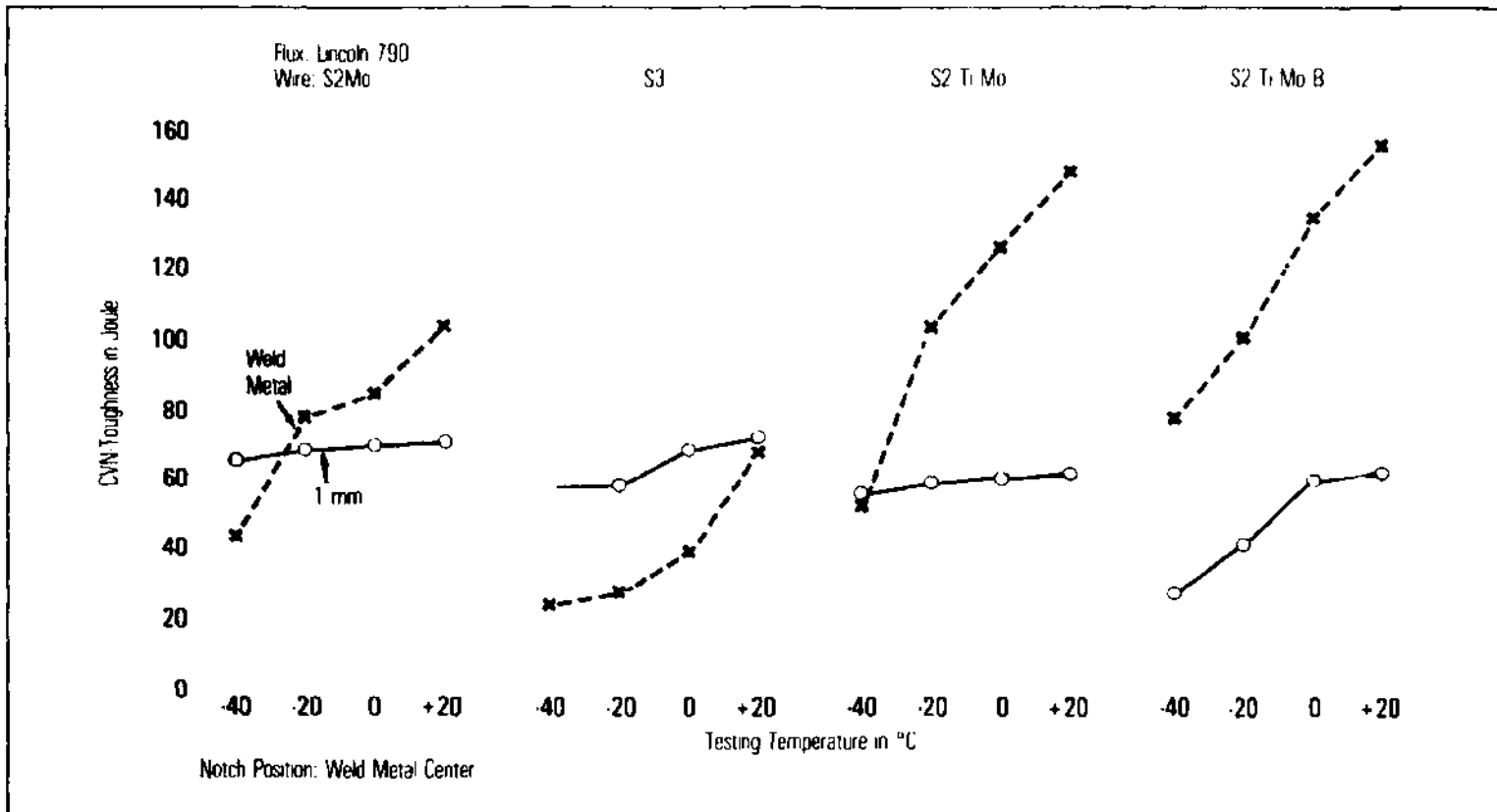


Fig. 23 — Toughness of Ni Nb spiral pipe weld metal for various wire composition (Laboratory Welding).

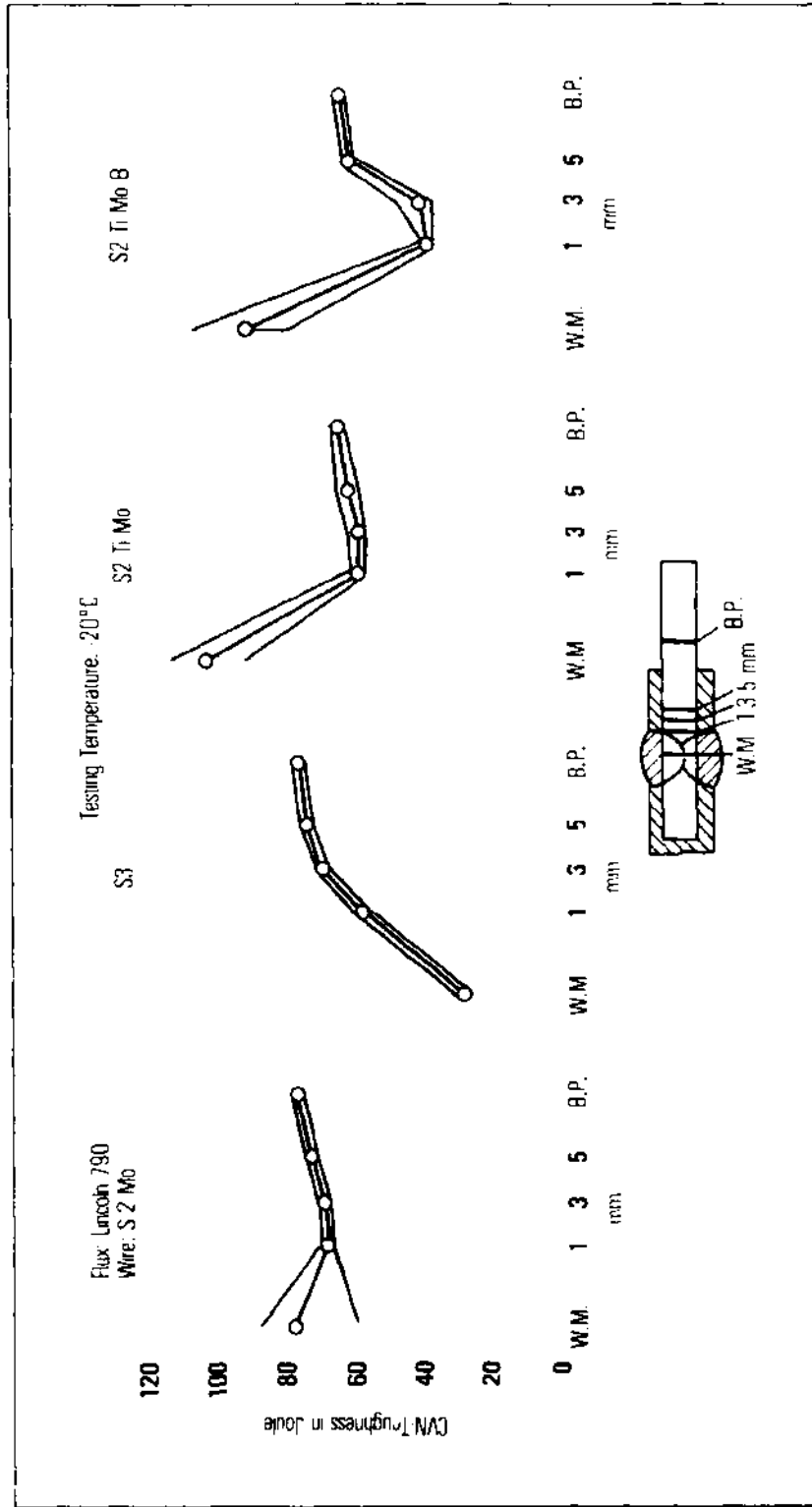


Fig. 24 — Toughness of Ni Nb spiral pipe weldment (16 mm) (Laboratory Welding).

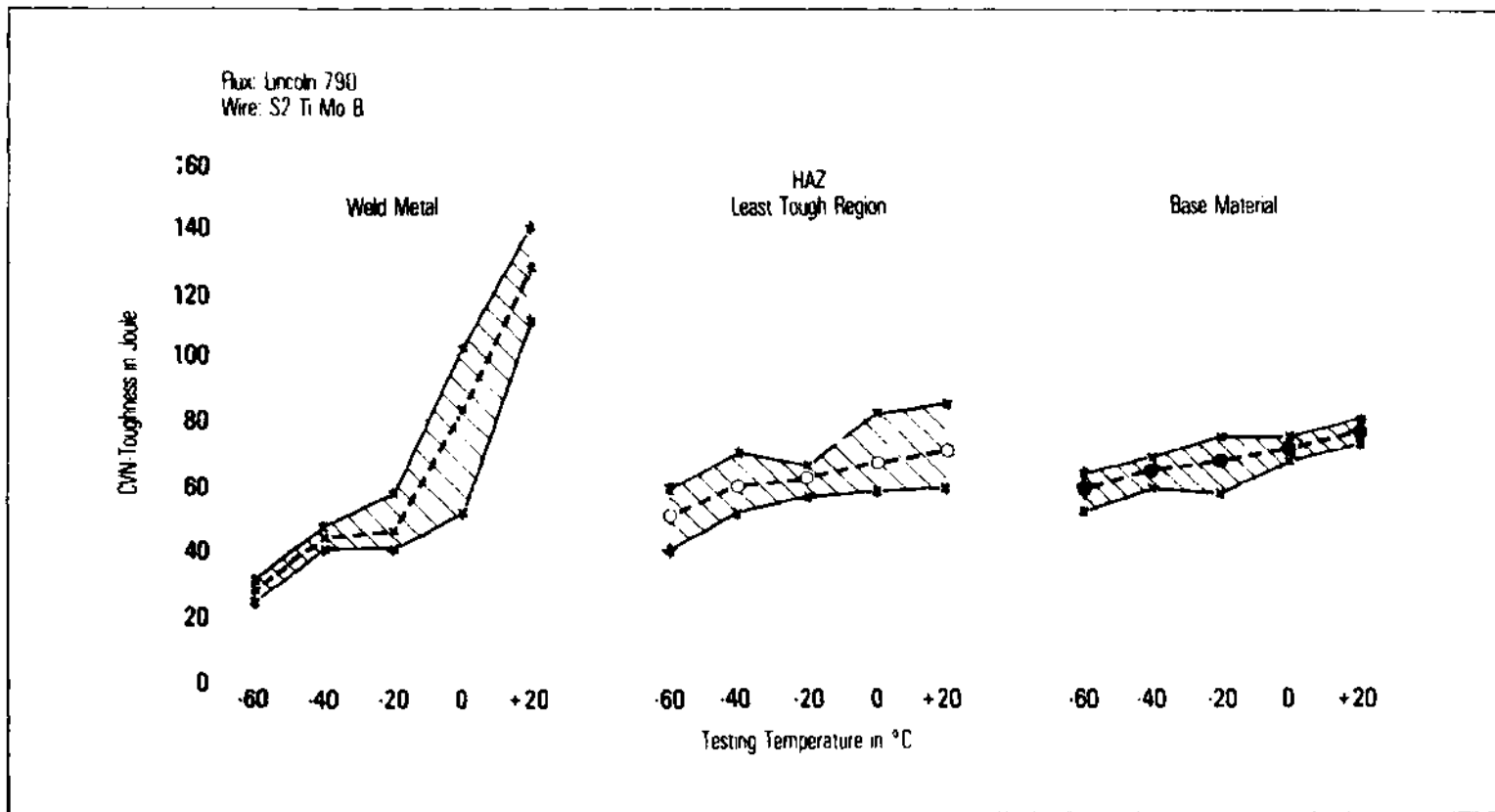


Fig. 25 — Toughness of Ni Nb spiral pipe.



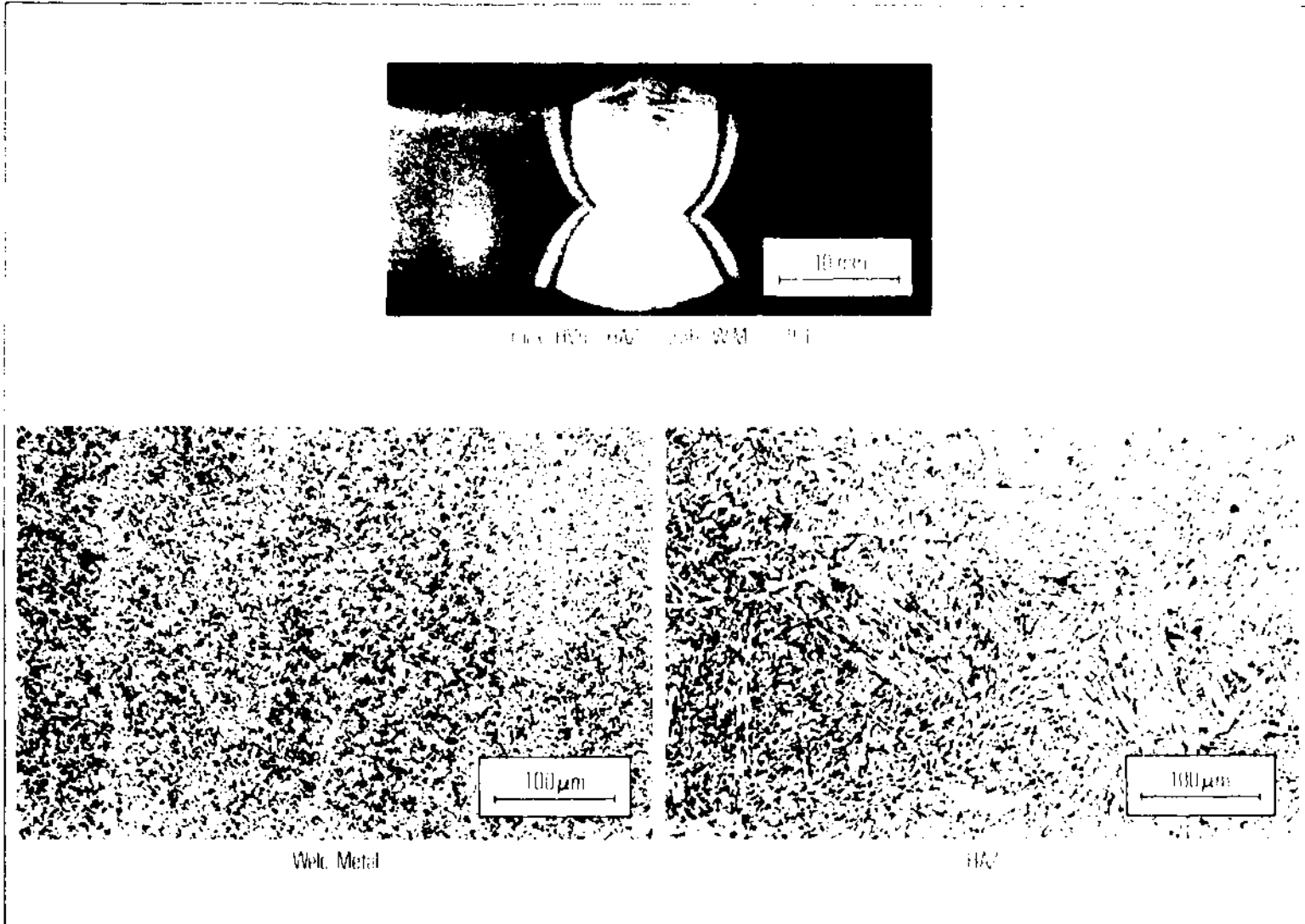


Fig. 26 — Microstructure of Ni Nb spiral pipe (S2 TiMoB wire, Lincoln 790 flux).

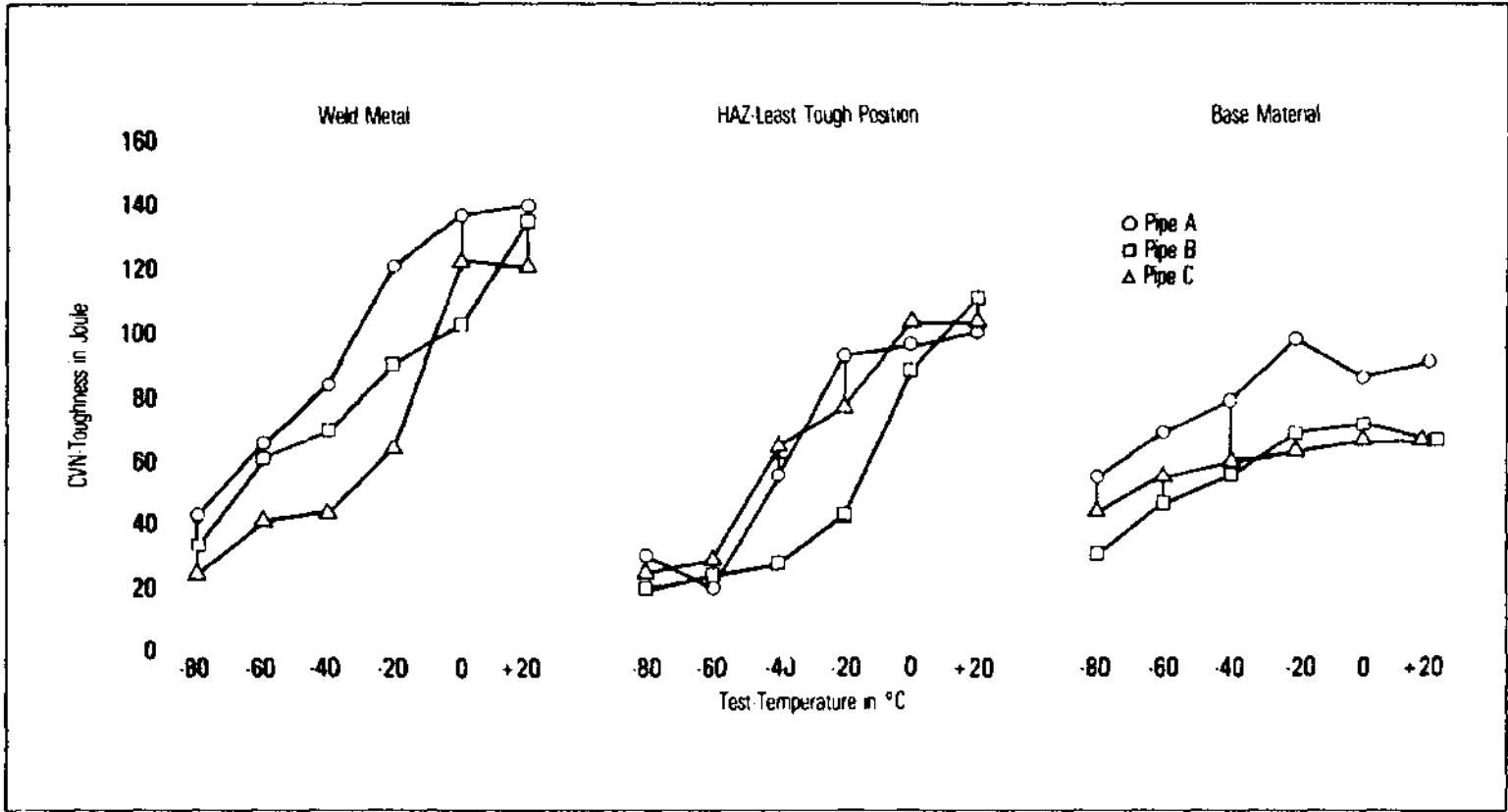


Fig. 27 — Toughness properties of Ni Nb - UO - pipes.

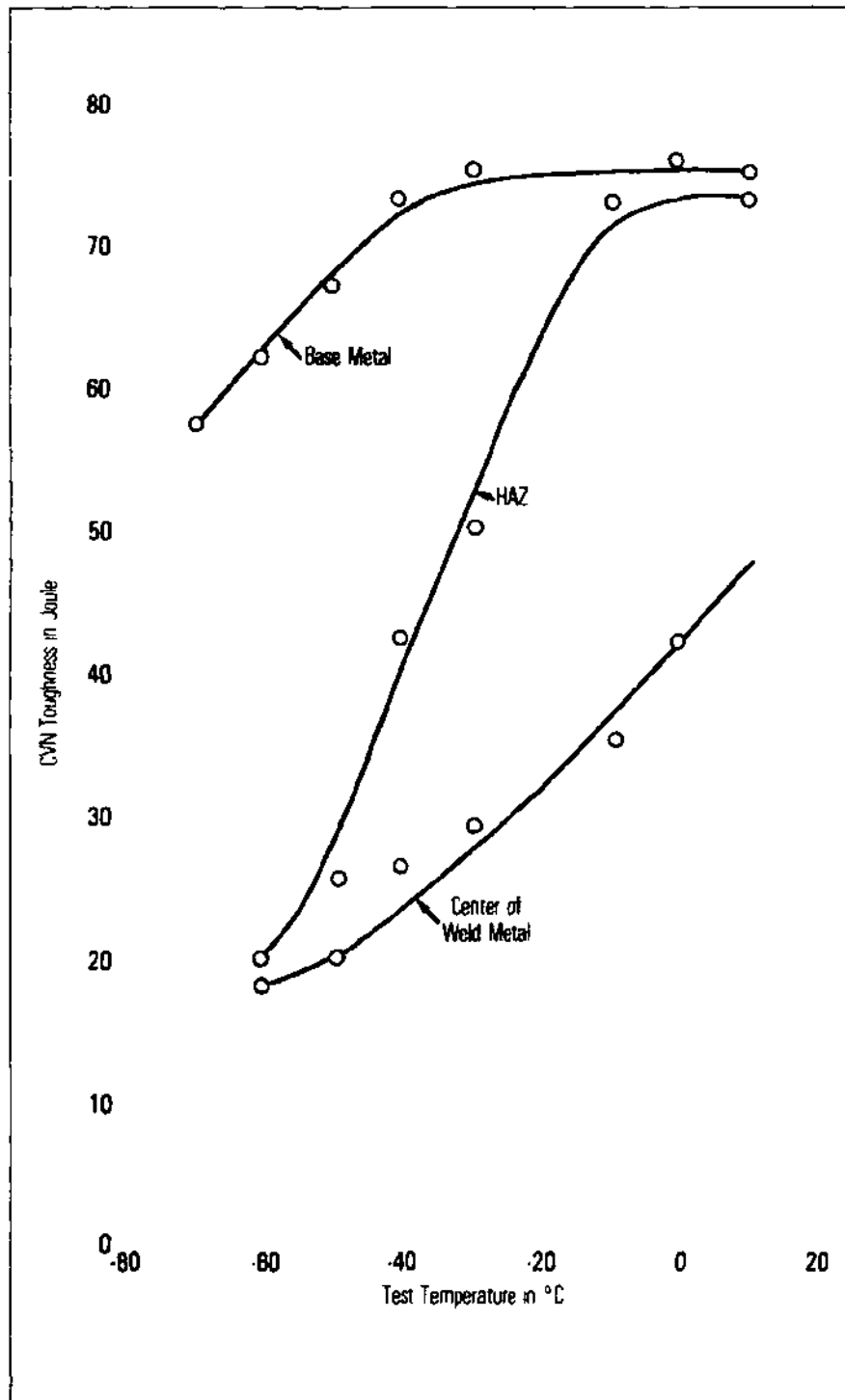


Fig. 28 — Toughness properties of Ni Nb - UO - pipe (56 Inch  $\times$  17.5 mm, transverse).

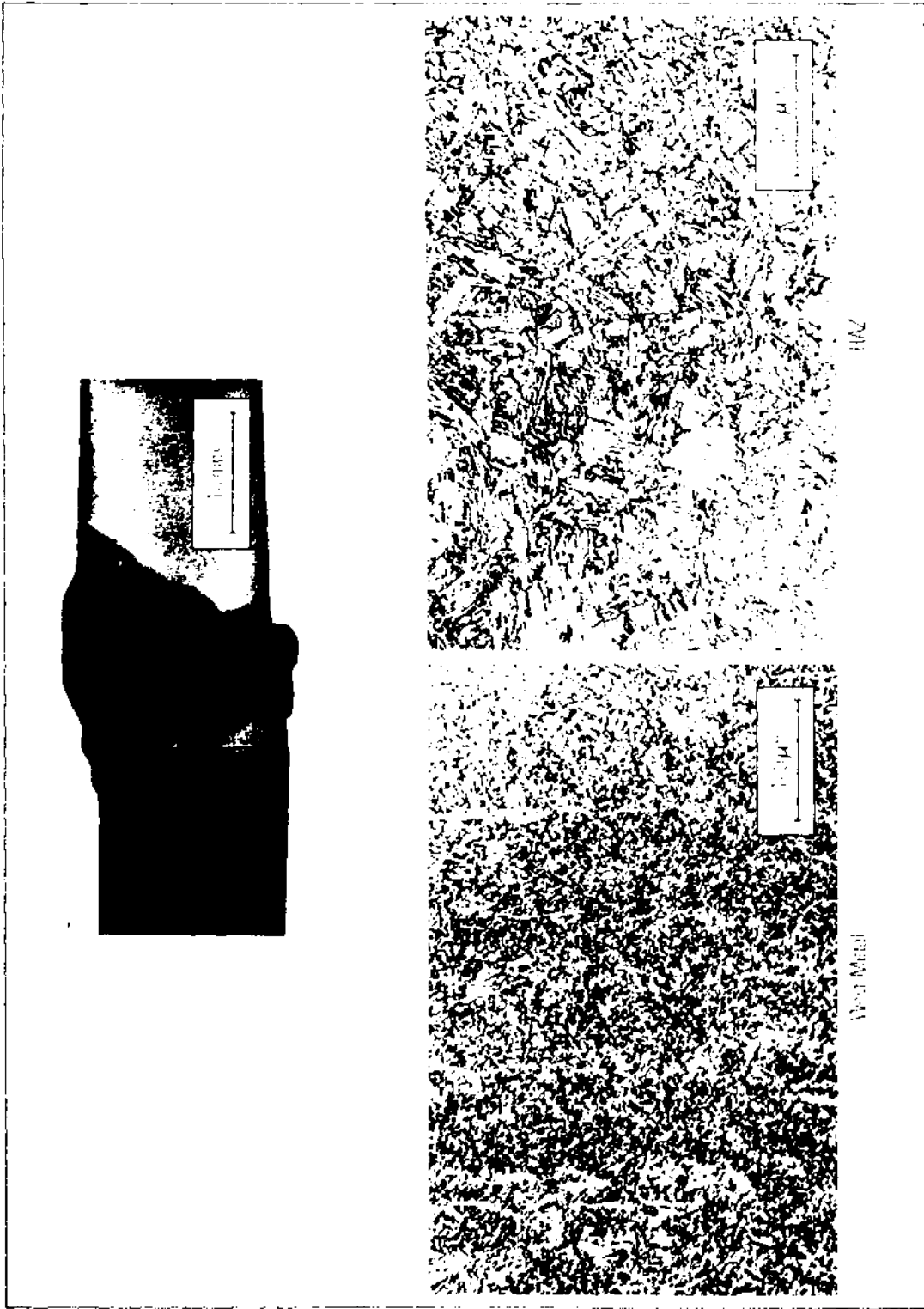


Fig. 29 — Microstructure of circumferential weldment of Ni Nb steel (spiral pipe).

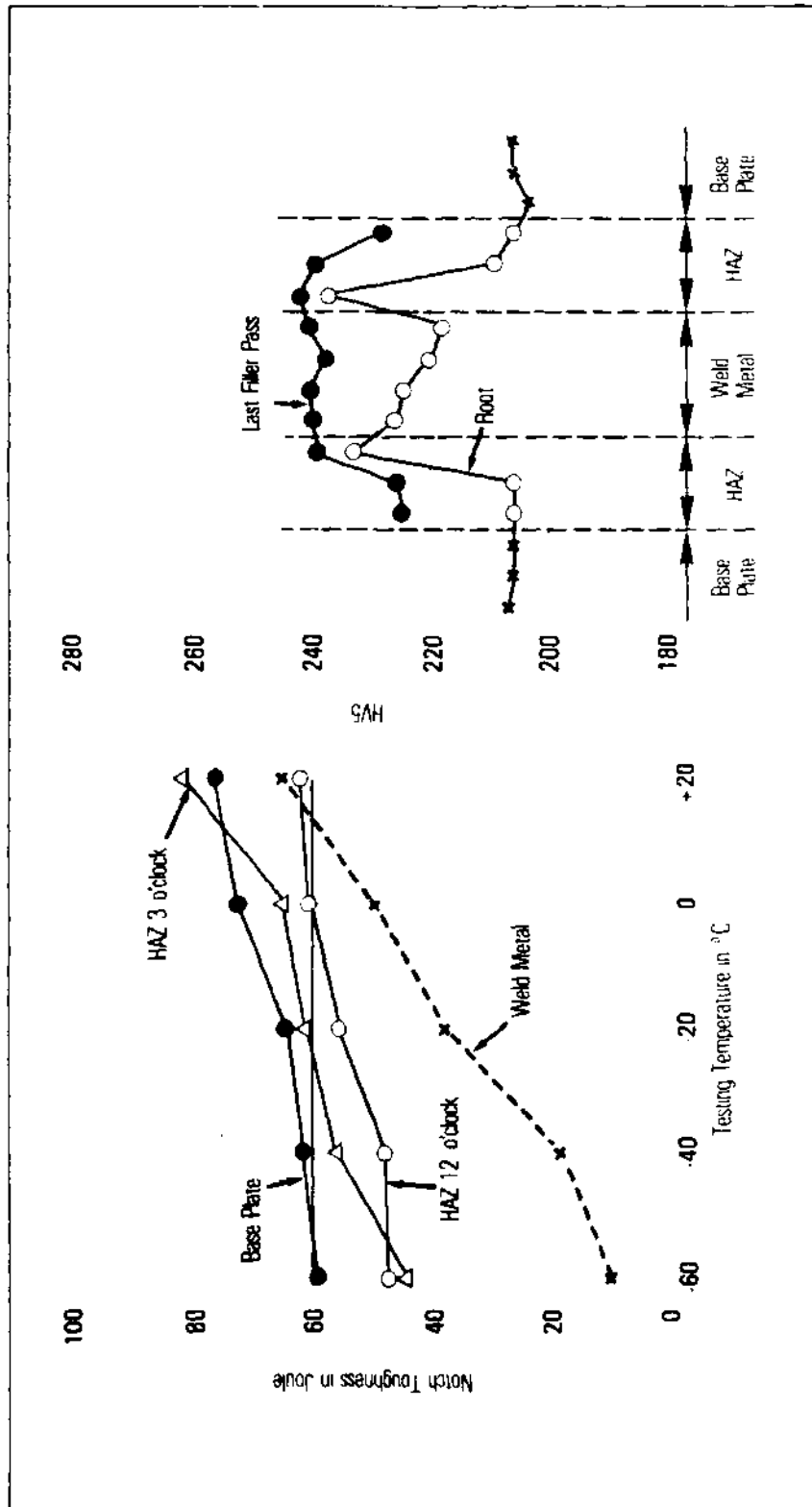


Fig. 30 — Notch toughness and hardness distribution in circumferential weldment of Ni Nb spiral pipe.

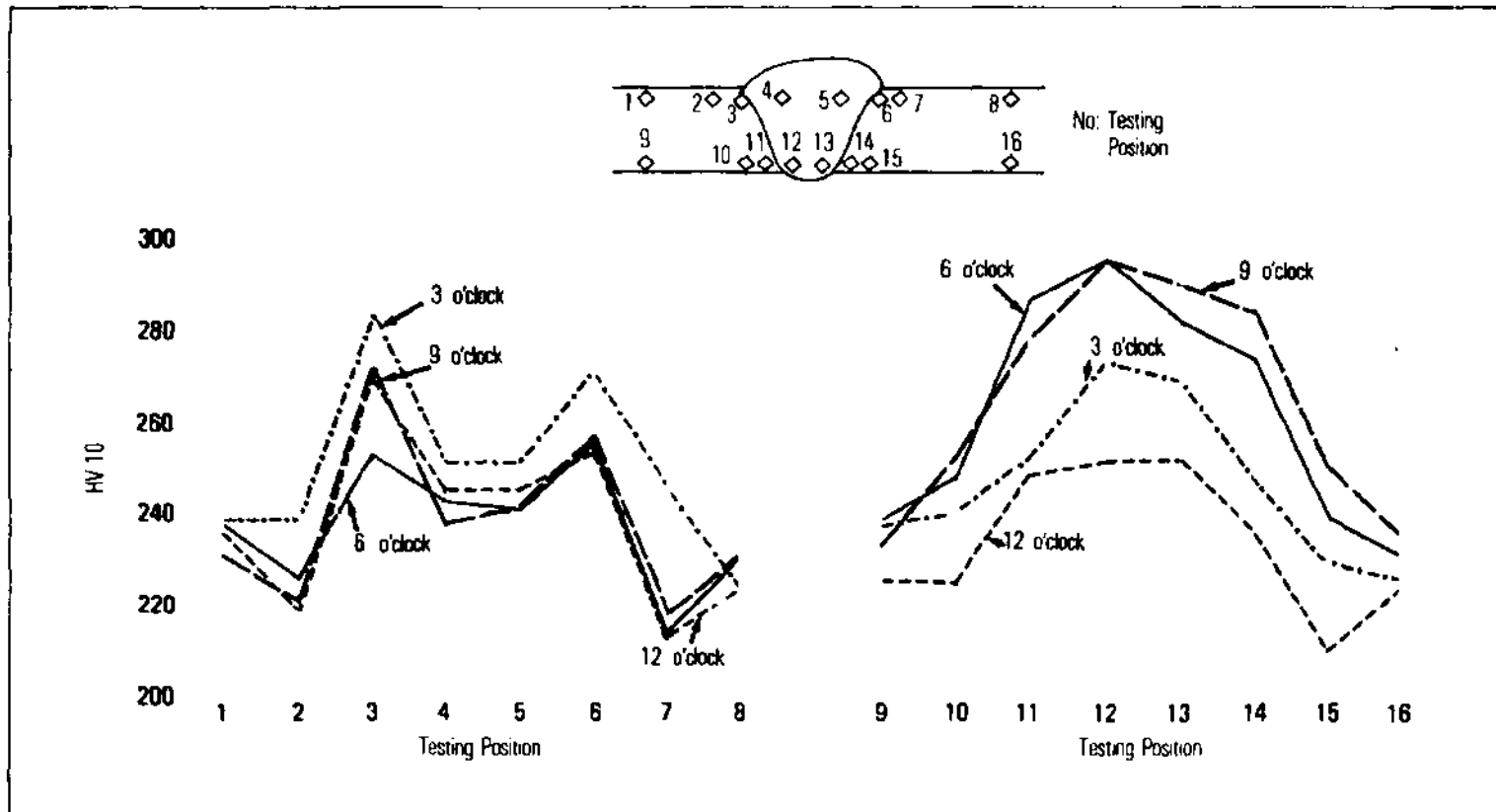


Fig. 31 — Hardness distribution in CRC-cross weldment of Ni Nb pipe (as welded).



**COMPANHIA BRASILEIRA DE  
METALURGIA E MINERAÇÃO**

---

CBMM is a Brazilian Corporation, engaged in mining, beneficiation and industrialization of the pyrochlore reserves located in Araxó, Minas Gerais. These reserves amount to 460 million tons of ore with a  $Nb_2O_5$  concentration of 2.5%. With a fully integrated operation, CBMM has amongst its main products standard and vacuum grade FeNb, NiNb and  $Ni_2O_3$ . Aiming at the development of new applications for niobium and at improving available technologies, CBMM maintains a very active R & D program which is being carried out in universities and research centres both in Brazil and abroad. The Niobium Information Centre (CITEN) located in São Paulo, is a cornerstone of that system - its mission is the dissemination of technical information about niobium.